Journal of Statistical Physics (2024) 191:27
https://doi.org/10.1007/s10955-024-03238-3

Irregular Gyration of a Two-Dimensional Random-Acceleration Process in a Confining Potential

Victor Dotsenko[1] · Gleb Oshanin[1] · Leonid Pastur[2,3] · Pascal Viot[1]

Received: 21 September 2023 / Accepted: 22 January 2024 / Published online: 23 February 2024

Abstract

We study the stochastic dynamics of a two-dimensional particle whose coordinates are described by two coupled one-dimensional random-acceleration processes, that evolve in a confining parabolic potential and are subject to independent Gaussian white noises with different amplitudes (temperatures). We first determine standard characteristics: the mixed moments of positions and velocities, as well as the position-velocity probability density function (PDF) and those of its kinetic and potential energies. Going then beyond these standard characteristics, we consider the emerging rotational motion of the particle around the origin: We show that if the amplitudes of the noises are not equal, the particle experiences a non-zero (on average) torque, such that the angular momentum L and the angular velocity W have non-zero mean values which both are (irregularly) oscillating with time t. We evaluate the PDF-s of L and W and show that the former has exponential tails for any fixed t, and hence, all moments. In the large-time limit this PDF converges to a uniform distribution with a diverging variance. The PDF of W possesses heavy power-law tails such that the mean W is the only existing moment. However, this PDF converges to a well-defined large-time limit manifesting the possibility of stabilizing phenomenon even in frictionless driven systems. Surprisingly, the limit is independent of the amplitudes of noises.

Communicated by Gregory Schehr.

✉ Pascal Viot
viot@lptmc.jussieu.fr

Victor Dotsenko
dotsenko@lptmc.jussieu.fr

Gleb Oshanin
gleb.oshanin@sorbonne-universite.fr

Leonid Pastur
pastur2001@yahoo.com

[1] Laboratoire de Physique Théorique de la Matière Condensée (UMR CNRS 7600), Sorbonne Université, 4 place Jussieu, Paris 75005, France

[2] B. Verkin Institute for Low Temperature Physics and Engineering, 47 Nauky Ave., Kharkiv 61103, Ukraine

[3] King's College London, Strand, London WC2R 2LS, UK

Keywords Random-acceleration process · Brownian gyrator model · Out-of-equilibrium dynamics · Spontaneous rotational motion

Contents

1 Introduction

When a physical system is brought in contact with several heat baths maintained at different temperatures, the whole system evolves towards a non-equilibrium steady-state characterized by a non-zero current and non-equilibrium fluctuations. One-dimensional solvable models have been developed to demonstrate this behavior [1–3] as well as the validity of fluctuation theorems and relations (see, e.g., [4–7]).

In higher dimensions, the Brownian gyrator model (BGM) provides an exactly solvable, albeit a minimalist example of a system that exhibits such a non-trivial non-equilibrium behavior. In d-dimensions the model consists of d linearly coupled one-dimensional Ornstein-Uhlenbeck (OU) processes (see, e.g., [8]) each with its own zero-mean Gaussian white noise that is statistically-independent of the noises of other components and is characterized by its own amplitude. In general, the amplitudes of the noises are not all equal to each other, and the amplitudes of the correlation function of noises (called in what follows, for simplicity, as the temperatures) do not obey the standard Einstein relations, i.e., are not simply proportional to the product of the bath temperature and the damping constant. This could require rather sophisticated methods for experimental realization of systems in question (see below).

The BGM was first introduced in [9] for the analysis of the emerging steady-state and its effective temperature in a system of two coupled single-spin paramagnets, each being in contact with its own thermal bath. Some years after, it was argued in [10] that, in fact, the BGM represents a minimal heat engine: there emerges a non-zero current which moreover has a non-zero curl, generating therefore a non-zero torque. As a result, if these d OU processes are used to describe the components of an instantaneous position of a particle living in a d-dimensional space, then the particle would "gyrate" around the origin, which explains the name of the model.

Various aspects of the dynamical and the steady-state behavior of the BGM have been analyzed in case of standard delta-correlated in time noises acting on the position components of

the particle (see, e.g., [11–20]) and also for the noises with long-ranged temporal correlations [21, 22]. The versions of the model that have been studied deal with the entropy production [23, 24], effects of anisotropic fluctuations [25, 26] and non-harmonic potentials [27], rotational dynamics of a Brownian ellipsoid in isotropic potential or of an inertial chiral ellipsoid [28], the spectral properties of individual trajectories of a gyrator [29, 30], emerging cooperative behavior of several Brownian gyrators [31, 32], as well as a synchronization of two out-of-equilibrium Kuramoto oscillators living at different temperatures [33]. By exerting an external force on the Brownian gyrator, it was possible to derive the asymmetry relations obeyed by the position probability density [34–36]. The probability densities of the gyration characteristics – the angular momentum and the angular velocity – have been evaluated in recent work [37], while in [38, 39] the moment-generating function of a time-averaged angular momentum has been studied within a somewhat different context.

The BGM, being clearly a minimalist model, is experimentally-realizable. In [11–13] the BGM was conceived by constructing an effective electric circuit comprising a capacitance and two resistors kept at different temperatures. In turn, in [40] the BGM was ingeniously devised very directly in a system with a single colloidal Brownian particle that is optically trapped in an elliptical potential well and coupled simultaneously to two heat baths with different temperatures acting along perpendicular directions. As we have already remarked, producing an effective coupling to two "heat baths" with different temperatures requires a special set-up. In particular, in [40] the isotropic thermal environment was made anisotropic via a fluctuating electric field with a near-white frequency spectrum applied along the x-direction. This electric fluctuating field was generated by two thin wires with electric white noise placed on either side of the optical trap and raised the bath noise temperature along the x-direction to 1750 K, while the bath noise temperature along the y-direction remained at 292 K (room temperature). Alternatively, in [13] the temperature difference has been achieved by imposing an additional noise on the position of the tweezer. In both experimental set-ups, noises not only with the temperatures that differ from the one of the thermal bath can be generated, but also noises with controlled long-ranged temporal correlations, such as, e.g., fractional Gaussian noise. Some additional realizations of the model have been mentioned in [10] and [16, 41, 42].

Most of available analytical analysis, with an exception of those in [16, 17], were concerned with the simplest case of a massless particle, i.e., the effects of inertia were discarded. While such effects were only briefly discussed in [16], a more systematic analysis was developed in [17] by using an appropriately generalized Langevin description and numerical simulations. The analysis in [17] evidenced some interesting effects of the inertia in the steady-state such as, e.g., a reduction of the non-equilibrium effects by diminishing the declination of the probability density and the mean value of a specific angular momentum. It was also demonstrated that rotation is maximized at a particular anisotropy while the stability of the rotation is minimized at a particular anisotropy or mass. We note, however, that the analysis in [16, 17] was focused exclusively on the behavior in the steady-state attained in the limit $t \to \infty$ just because of the dissipation due to the friction term $\gamma \dot{x}$ in the corresponding dynamical equation.

In this paper we study a two-dimensional BGM with inertia and, in contrast to [16, 17] which analyzed solely the behavior in the steady-state, we concentrate here on the *temporal* evolution of the standard characteristic properties, such as, e.g., positions, velocities, their mixed moments and their full probability density functions (PDF)s, as well as on the characteristics of the emerging gyration process; that being, the angular momentum L and the angular velocity W. To get the understanding of possible effects of the inertia, and to make our analysis more transparent and the corresponding effects more pronounced, we

exclude the friction term, hence, the dissipation. In fact, we assume the validity of the strong inequality $m \gg \gamma t$ between the particle, the friction constant and the time of evolution. An experimental realization of this set-up could be the one similar to that in [40], i.e., dealing with a massive colloidal particle placed in a low-viscosity fluid. In this case our model will describe the transient behavior of the particle.

We note that this simplified case is also of interest from a purely mathematical perspective: In our situation one deals with two coupled one-dimensional random-acceleration processes, each living at its own temperature and both evolving in a parabolic potential. The random-acceleration process, mainly in one-dimensional systems, has received much interest within the last decade as a simple example of a super-diffusive non-Markovian stochastic process which exhibits ageing and a non-trivial behavior of the extremal properties [43–50]. Moreover, this process appears in rather diverse contexts in physical systems. To name a few, we mention dynamics of a granular particle in presence of an inelastic wall [51–54], the short-time dynamics of active particles as observed for different kinds of microorganisms [55, 56] or in active trap model [57, 58], decaying turbulence in Burgers equation [59], particle motion in a sheared medium [60], as well conformational statistics of semi-flexible polymer chains in narrow channels [61, 62].

Returning to our case, we note that, not counter-intuitively, the dynamics of our system shows a completely different behavior as compared to that of the standard BGM. In the absence of dissipation, an ongoing pumping of energy delocalizes the particle such that its mean-squared distance from the origin grows linearly with time, while for the BGM it tends to a constant as $t \to \infty$. As a consequence, the steady state does not exist. On average, the particle still performs a rotational motion (likewise the BGM) when the temperatures of the components are not equal to each other and when the confining potential is anisotropic, but it gradually travels away from the origin. The temporal evolution of the characteristic properties of the gyration process is also strikingly different from that of the standard BGM. In particular, the mean angular moment (which approaches a constant value for the BGM) in our case oscillates with time between its maximal and minimal values which have different signs. Correspondingly, the torque imposed on the particle also oscillates prompting the particle to rotate clockwise and counter-clockwise at different time intervals. The time-averaged mean angular momentum approaches nonetheless a constant value as $t \to \infty$, such that the particle eventually gyrates around the origin, on average, and the gyration direction is defined solely by the relation between the temperatures of the components. Accordingly, the mean angular velocity is an oscillatory function of time, and the amplitude of oscillations decreases as the first inverse power of time due to an displacement of the particle away from the origin.

Further on, motivated by the analysis in recent work [37], we calculate the full probability densities of the angular momentum and the angular velocity. We find that, at a finite time t, the probability density of the angular momentum has exponential tails and hence, all moments are finite. However, this distribution is effectively broad and its variance diverges with t as t^2, while the expectation is bounded in t. This signifies that the expectation does not bear significant physical information and only indicates a certain non-zero trend (once the temperatures of the components are unequal) in an ensemble of the processes under study rather than the behavior to be observed for each individual realization. Thus, the complete description of such strongly fluctuating observables is given only by their probability distribution. This is, in particular, clear for the observables with infinite second moment. We show that this is the case for the angular velocity whose probability density has heavy power-law tails so that the mean angular velocity is the only finite moment. Curiously enough, in the limit $t \to \infty$, the probability density of the angular velocity converges to a remarkably simple limiting form which is completely independent of the temperatures of the components. Therefore,

one observes quite a non-trivial irregular behavior of the angular momentum and the angular velocity as functions of time, with quite significant fluctuations.

The paper is organized as follows: in Sect. 2, we formulate the model and introduce basic notations. In Sect. 3 we concentrate on the moments and the cross-moments of the particle's position and velocities, while in Sect. 4 we discuss the behavior of the two-time correlation function of the particle's position. Section 5 is devoted to the position-velocity probability densities. In Sect. 6 we focus on the gyration characteristics, i.e., the angular momentum and the angular velocity. We derive explicit expressions for the mean values of these characteristic properties and also their full probability densities. We analyze the statistical properties of the kinetic, potential and total energy in Sect. 7.

Finally, in Sect. 8 we conclude with a brief recapitulation of our results and a short discussion.

2 The Model

We consider the dynamics of a particle of mass m in a two-dimensional system, in the presence of a potential that consists of two parts:

(i) The confining potential which we assume, following the trend of the field, to be the paraboloid

$$U(x,y) = \lambda\Big(\frac{1}{2}x^2 + \frac{1}{2}y^2 + u\,xy\Big), \tag{1}$$

where $\lambda > 0$ controls the amplitude of attraction to the origin (e.g., the strength of an optical trap), while u is the (relative to λ) coupling parameter between the x- and y-components. We assume that $|u| < 1$, to guarantee that U is a paraboloid and hence, that $\exp(-U)$ is integrable.

(ii) The additive random "potential"

$$\Xi(x,y,t) = x\xi_1(t) + y\xi_2(t), \tag{2}$$

where $\xi_1(t)$ and $\xi_2(t)$ are mutually-independent stochastic noises with zero mean and the covariances

$$\begin{aligned}\big\langle \xi_x(t')\xi_x(t)\big\rangle &= 2T_1\delta(t-t'),\\ \big\langle \xi_y(t')\xi_y(t)\big\rangle &= 2T_2\delta(t-t').\end{aligned} \tag{3}$$

The angle brackets in Eqs. (3) denote averaging with respect to realizations of thermal noises, and T_1 and T_2 are the respective "temperatures" of the two thermal baths, (which are in general unequal). We will characterize the situation as equilibrium or non-equilibrium in cases where $T_1 = T_2$ or $T_1 \neq T_2$ respectively.

Denoting by $\mathbf{r}(t) = (x(t),\ y(t))$ the instantaneous coordinates of the particle, we can write down its equation of motion as[1]

$$\begin{aligned} m\,\ddot{x}(t) + \lambda x(t) + \lambda u y(t) &= \xi_1(t),\\ m\,\ddot{y}(t) + \lambda y(t) + \lambda u x(t) &= \xi_2(t).\end{aligned} \tag{4}$$

[1] Recall that in the standard BGM one has the first derivatives of the position components $x(t)$ and $y(t)$ with respect to time, in place of terms $m\ddot{x}(t)$ and $m\ddot{y}(t)$, i.e;

$$\nu\,\dot{x}(t) + \lambda x(t) + \lambda u y(t) = \xi_1(t), \qquad \nu\,\dot{y}(t) + \lambda y(t) + \lambda u x(t) = \xi_2(t),$$

where ν is the damping constant and the potential is defined in Eq. (1).

To define uniquely the dynamics we have to add the initial conditions. We will be mostly interested by the large-time dynamics of the particle due to the presence of the noise, and hence, it seems quite natural to assume, for simplicity, that the particle starts from the very bottom of the confining potential. Without any significant lack of generality, we also stipulate that the particle's velocity is equal zero at time $t = 0$. Therefore, Eqs. (4) are to be solved subject to the initial conditions

$$\begin{aligned} x(0) = y(0) = 0, \\ \dot{x}(0) = \dot{y}(0) = 0. \end{aligned} \tag{5}$$

The general case of non-zero initial conditions can be easily obtained from the case (5) by replacing $\mathbf{r}(t)$ above by $\mathbf{r}(t) + \mathbf{r}_0(t)$, where $\mathbf{r}_0(t)$ is the standard linear combination of simple harmonic functions, the solution of Eqs. (4) with given initial conditions and zero right-hand-side (r.h.s).

There are several properties of focal interest, which characterize the stochastic process defined in Eqs. (3) – (5). First of all, these are the moments of instantaneous positions $x(t)$ and $y(t)$ and the velocities $\dot{x}(t)$ and $\dot{y}(t)$, as well as their mixed moments. More generally, this is the joint position-velocity probability density $P_t = P_t(x, y, \dot{x}, \dot{y})$. Taking into account that Ξ of Eqs. (2)–(3) is a pair of independent white noises, the collection

$$\mathbf{X} = \{X_j\}_{j=1}^4 = \{x, y, \dot{x}, \dot{y}\} \tag{6}$$

forms a four component Markov process, hence, their P_t solves the corresponding Fokker-Planck equation. This proved to be a fairly efficient and adequate tool in the case of non-linear dynamics and/or non Gaussian but Markovian Ξ (see e.g. [63]), where the collection $\{X, \Xi\}$ forms a Markov process. In our case of linear dynamics and Gaussian white noise Ξ of Eqs. (2)–(3) the collection, Eq. (6), is also Gaussian. In addition it follows from Eqs. (3) to (5) that

$$\langle X_j(t) \rangle = 0, \;\; j = 1, 2, 3, 4. \tag{7}$$

Thus, it suffices to find the (covariance) matrix of $X(t)$,

$$\begin{aligned} M(t) = \{m_{jk}\}_{j,k=1}^4, \;\; m_{jk} = \langle X_j(t) X_k(t) \rangle, \\ M(t) = \begin{pmatrix} \langle x^2(t) \rangle & \langle x(t)y(t) \rangle & \langle x(t)\dot{x}(t) \rangle & \langle x(t)\dot{y}(t) \rangle \\ \langle x(t)y(t) \rangle & \langle y^2(t) \rangle & \langle y(t)\dot{x}(t) \rangle & \langle y(t)\dot{y}(t) \rangle \\ \langle x(t)\dot{x}(t) \rangle & \langle y(t)\dot{x}(t) \rangle & \langle \dot{x}^2(t) \rangle & \langle \dot{x}(t)\dot{y}(t) \rangle \\ \langle x(t)\dot{y}(t) \rangle & \langle y(t)\dot{y}(t) \rangle & \langle \dot{x}(t)\dot{y}(t) \rangle & \langle \dot{y}^2(t) \rangle \end{pmatrix}, \end{aligned} \tag{8}$$

to be able to obtain its characteristic function

$$\Phi_t(\boldsymbol{\omega}) = \int_{\mathbb{R}^4} e^{i(\boldsymbol{\omega}, \mathbf{X})} \, P_t(\mathbf{X}) d\mathbf{X} = \exp\{-(M(t)\boldsymbol{\omega}, \boldsymbol{\omega})/2\}, \tag{9}$$

where $\boldsymbol{\omega} = \{\omega_j\}_{j=1}^4$ are the Fourier components of the position and velocity. $(\boldsymbol{\omega}, \mathbf{X})$ denotes the dot product between the two vectors.

Likewise, the corresponding joint probability distribution density P_t of $\mathbf{X}$ is, in general

$$P_t(X) = ((2\pi)^4 \det M(t))^{-1/2} \exp\{-(M^{-1}(t)X, X)/2\}. \tag{10}$$

However, for this formula to be well defined, the covariance matrix (8) has to admit the inverse matrix $M^{-1}(t)$. It follows from the results of Sections 3.1–3.2 that the leading terms

of the large-t asymptotics of the diagonal entries of $M(t)$ are proportional to t, while the off-diagonal entries are bounded in t. This implies the invertibility of $M(t)$ if t is large enough. A more sophisticated argument shows that $M(t)$ is invertible for any $t > 0$ (see Appendix A).

The knowledge of Φ_t or/and P_t allows one to study the behavior of two important quantities that characterize, as in the case of the BGM, the emerging rotational motion of the particle.

The first is its angular momentum

$$\mathbf{L}(t) = m\mathbf{r}(t) \times \mathbf{v}(t), \ \ \mathbf{v}(t) = \dot{\mathbf{r}}(t), \tag{11}$$

where $\mathbf{r}(t) \times \mathbf{v}(t)$ is the cross product of the position and the velocity of the particle, so that $\mathbf{L}$ is perpendicular to the plane of motion

$$\mathbf{L}(t) = (0, 0, L), \ \ L(t) = m\left(x(t)\dot{y}(t) - y(t)\dot{x}(t)\right). \tag{12}$$

The second characteristic of interest is the angular velocity, which is formally defined as

$$\mathbf{W}(t) = (0, 0, W(t)), \ \ W(t) = \frac{x(t)\dot{y}(t) - y(t)\dot{x}(t)}{x^2(t) + y^2(t)}. \tag{13}$$

We will study below certain moments of these random variables, and will also derive exact expressions for their probability densities.

Lastly, to simplify the subsequent formulas, we set $m = 1$ in what follows. The dependence of m can be easily recovered in our final results by simply multiplying $L(t)$ and $W(t)$ by m, by replacing λ by λ/m, and the temperatures $T_{1,2}$ by $T_{1,2}/m^2$.

3 Particle's Trajectories and Velocities, and Their Moments

We will omit the argument t in many functions below where this does not lead to a confusion.

The solution of the system of two ordinary linear differential equations (4) with constant coefficients for the initial conditions in Eqs. (5) and a fixed realization of noises, Eqs. (2) and (3), is obtained by standard method and is (see also Appendix A for its another form): is

$$\begin{aligned} x = x(t) &= \frac{1}{2}\int_0^t d\tau \Big[Q_+(t-\tau)\xi_1(\tau) + Q_-(t-\tau)\xi_2(\tau) \Big], \\ y = y(t) &= \frac{1}{2}\int_0^t d\tau \Big[Q_-(t-\tau)\xi_1(\tau) + Q_+(t-\tau)\xi_2(\tau) \Big], \end{aligned} \tag{14}$$

where we denoted

$$Q_\pm(t) = \frac{\sin(\Omega_+ t)}{\Omega_+} \pm \frac{\sin(\Omega_- t)}{\Omega_-}, \quad \Omega_\pm = \sqrt{\lambda(1 \pm u)}, \ \ |u| < 1. \tag{15}$$

In turn, differentiating Eqs. (14) and (15) with respect to time, we find the instantaneous velocities $\dot{x}(t)$ and $\dot{y}(t)$:

$$\begin{aligned} \dot{x} = \dot{x}(t) &= \frac{1}{2}\int_0^t d\tau \Big[\dot{Q}_+(t-\tau)\xi_1(\tau) + \dot{Q}_-(t-\tau)\xi_2(\tau) \Big], \\ \dot{y} = \dot{y}(t) &= \frac{1}{2}\int_0^t d\tau \Big[\dot{Q}_-(t-\tau)\xi_1(\tau) + \dot{Q}_+(t-\tau)\xi_2(\tau) \Big], \end{aligned} \tag{16}$$

with

$$\dot{Q}_\pm(t) = \cos(\Omega_+ t) \pm \cos(\Omega_- t). \tag{17}$$

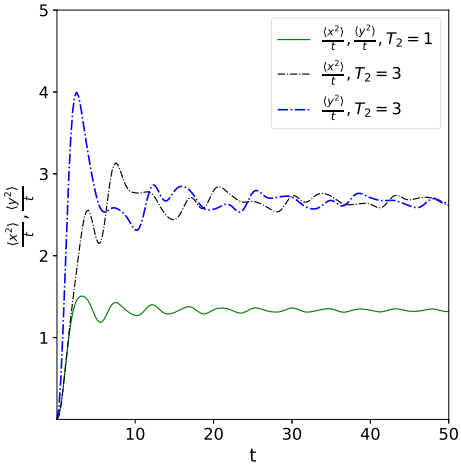

Fig. 1 Reduced position moments $\langle x^2\rangle/t$ and $\langle y^2\rangle/t$ versus time for $T_1 = 1$ and $T_2 = 1$ and $T_2 = 3$

We will analyze now the behavior of the moments of the instantaneous positions and velocities.

3.1 Second Moments of Positions

Explicit expressions for the mean-squared displacements from the origin follow readily from Eqs. (14) and (15):

$$\begin{aligned}\langle x^2\rangle = &\frac{(T_1+T_2)}{2\lambda(1-u^2)}\,t - \frac{(T_1+T_2)}{8}\left(\frac{\sin(2\Omega_+ t)}{\Omega_+^3} + \frac{\sin(2\Omega_- t)}{\Omega_-^3}\right)\\ &+ \frac{(T_1-T_2)}{2u\lambda}\left[\frac{\cos(\Omega_- t)\sin(\Omega_+ t)}{\Omega_+} - \frac{\cos(\Omega_+ t)\sin(\Omega_- t)}{\Omega_-}\right],\end{aligned} \tag{18}$$

and the expression of $\langle y^2\rangle$ is obtained from Eq.(18) by exchanging the temperatures $T_1 \leftrightarrow T_2$.

We observe that $\langle x^2\rangle$ and $\langle y^2\rangle$ differ only if $T_1 \neq T_2$ ("non-equilibrium" situation) as they should. The corresponding terms are proportional to $T_1 - T_2$ and are denoted here and below by square brackets. The leading large-t behavior of $\langle x^2\rangle$ and similarly $\langle y^2\rangle$ is identical and comes from the first terms in Eq. (18) which grow linearly with t. In the absence of friction, the harmonic force does not compensate the random force and progressively the particle moves at larger and larger distances with time. The signature of an oscillatory behavior appears in the two subdominant terms which remain bounded and exhibit irregular oscillations, due to the fact that the frequencies $\Omega_\pm$ are continuous functions of λ and u, hence, are incommensurate generically.

Fig. 1 shows the time evolution of the reduced moments $\langle x^2\rangle/t$ and $\langle y^2\rangle/t$ for $T_1 = 1$ and $T_2 = 1$ and 3. For $T_2 = T_1$, the reduced moments coincide, as they should. Approach to their asymptotic values is governed by oscillatory subleading terms. For $T_2 \neq T_1$, $\langle x^2\rangle/t$ and $\langle y^2\rangle/t$ converge to the same asymptotic value $(T_1 + T_2)/(2\lambda(1-u^2))$, but their behaviors at the intermediate times are very different.

It is also worth mentioning that in the limit $\lambda \to 0$, in which the potential in Eq. (1) vanishes, Eq.(18) predicts a much faster growth

$$\langle x^2 \rangle = \frac{2T_1}{3}\, t^3, \quad \langle y^2 \rangle = \frac{2T_2}{3}\, t^3, \quad \lambda = 0, \tag{19}$$

which is a well-known result for the random-acceleration process [43–49] (see also recent [50] and references therein). In addition, for $u = 0$, when the coordinates decouple, while $\lambda > 0$, we have two independent random-acceleration processes evolving in a quadratic potential. In this case, we get from Eq. (18)

$$\begin{aligned} \langle x^2 \rangle &= \frac{T_1}{\lambda}\, t - \frac{T_1}{2\lambda^{3/2}} \sin\left(2\sqrt{\lambda}t\right), \\ \langle y^2 \rangle &= \frac{T_2}{\lambda}\, t - \frac{T_2}{2\lambda^{3/2}} \sin\left(2\sqrt{\lambda}t\right), \quad u = 0, \quad \lambda > 0, \end{aligned} \tag{20}$$

i.e., that the mean square displacements increase linearly with time and have additional oscillating terms, whose frequency is determined by the amplitude of the potential.

Therefore, at long times the behavior of both $\langle x^2 \rangle$ and $\langle y^2 \rangle$ is effectively "diffusive". This does not imply, of course, that the processes $x(t)$ and $y(t)$ are standard Brownian motions but rather signifies that such a behavior results from an interplay between an ongoing input of energy (leading to a super-diffusive motion, Eq. (19)) and the restoring force due to the confining potential, which partially counter-balance each other. Indeed, one notices that because of this trade-off the prefactors in the leading terms in Eq. (18) is proportional to the sum of the temperatures, and are inversely proportional to λ. In Sect. 4 we will discuss the ageing behavior of the process $x(t)$ as embodied in its two-time covariance $\langle x(t)x(t_1)\rangle$, which manifests significant departures from the standard Brownian motion.

Lastly, we find the mixed moment $\langle xy \rangle$ of the components of instantaneous position. Using our Eqs. (14) and (15), we find that for any $t > 0$

$$\langle xy \rangle = -\frac{u\ (T_1 + T_2)}{2\lambda(1-u^2)}\, t - \frac{(T_1 + T_2)}{8} \left(\frac{\sin(2\Omega_+ t)}{\Omega_+^3} - \frac{\sin(2\Omega_- t)}{\Omega_-^3} \right), \tag{21}$$

We observe that the covariance depends only on the sum of the temperatures, unlike the moments $\langle x^2 \rangle$ and $\langle y^2 \rangle$ in Eq. (18). The leading large- t term of Eq. (21) grows linearly with time and its sign is opposed to that of the coupling parameter u and the sub-leading term oscillates irregularly.

3.2 Second Moments of Velocities and Velocity-Position Correlations

The second moments of the velocities $\dot{x}(t)$ and $\dot{y}(t)$ can be straightforwardly evaluated from our Eqs. (16) and (17). Skipping the details of the intermediate calculations, we get

$$\begin{aligned} \langle \dot{x}^2 \rangle = {} & \frac{(T_1 + T_2)}{2}\, t + \frac{(T_1 + T_2)}{8} \left(\frac{\sin(2\Omega_+ t)}{\Omega_+} + \frac{\sin(2\Omega_- t)}{\Omega_-} \right) \\ & + \frac{(T_1 - T_2)}{2u\lambda} \Big[\Omega_+ \cos(\Omega_- t) \sin(\Omega_+ t) - \Omega_- \cos(\Omega_+ t) \sin(\Omega_- t) \Big], \end{aligned} \tag{22}$$

and $\langle \dot{y}^2 \rangle$ is obtained from of Eq.(22) upon a replacement $T_1 \leftrightarrow T_2$.

We see that in the long time limit fluctuations of the velocities grow "diffusively", i.e., the second moments of velocities increase in proportion to the first power of time. The transient terms, important at the intermediate stages, exhibit irregular oscillations, because

the frequencies $\Omega_{\pm}$ are incommensurate generically. Such an ultimate diffusive growth is very similar (apart of a dimensional prefactor) to the one which we have previously observed for the second moments of $x(t)$ and $y(t)$ (see Eqs. (18)). There is, however, an important difference in the behavior of the moments of the position and those of the velocities. Namely, consider the limit $\lambda \to 0$, in which case the potential vanishes and $x(t)$ and $y(t)$ are standard independent random-acceleration processes that display a strongly super-diffusive behavior, (see Eq. (19)). Setting $\lambda = 0$ in Eq. (22) we get

$$\langle \dot{x}^2 \rangle = 2T_1\, t, \quad \langle \dot{y}^2 \rangle = 2T_2\, t, \quad \lambda = 0. \tag{23}$$

Next, for $\lambda > 0$ but $u = 0$, when the components $x(t)$ and $y(t)$ are two decoupled random-acceleration processes evolving each in a quadratic potential, Eq. (22) yields

$$\langle \dot{x}^2 \rangle = T_1\, t + \frac{T_1}{2\lambda^{1/2}} \sin\left(2\sqrt{\lambda} t\right) \quad u = 0,\ \lambda > 0., \tag{24}$$

and $\langle \dot{y}^2 \rangle$ is obtained by switching $T_1 \leftrightarrow T_2$ in Eq. (24). We conclude that the diffusive growth of fluctuations of velocities is a universal feature independent of the fact whether the potential in Eq. (1) is present or not, while the fluctuations of positions themselves behave very differently depending whether potential is present or not.

Further on, we find that the covariance $\langle \dot{x}\, \dot{y} \rangle$ of the components of velocities is given by

$$\langle \dot{x}\, \dot{y} \rangle = \frac{(T_1 + T_2)}{8\sqrt{\lambda(1-u^2)}} \left(\frac{\sin(2\Omega_+ t)}{\Omega_+} - \frac{\sin(2\Omega_- t)}{\Omega_-} \right), \tag{25}$$

hence, do not grow with time (unlike the correlations of positions, Eq. (21)), and oscillate around zero. The right-hand-side of Eq. (25) vanishes, as it should, when $\lambda \to 0$ or $u \to 0$.

Consider next the covariance of positions and velocities. One readily finds

$$\begin{aligned} \langle x\dot{x} \rangle = \frac{1}{2}\frac{d\langle x^2 \rangle}{dt} = \frac{(T_1 + T_2)}{4} \left(\frac{\sin^2(\Omega_+ t)}{\Omega_+^2} + \frac{\sin^2(\Omega_- t)}{\Omega_-^2} \right) \\ - \frac{(T_1 - T_2)}{2\lambda} \sin(\Omega_+ t) \sin(\Omega_- t)\,, \end{aligned} \tag{26}$$

and $\langle y\dot{y} \rangle$ is obtained by switching $T_1 \leftrightarrow T_2$ in Eq.(26).

Thus, the position-velocity covariances consist of two terms: the first one, which is proportional to the sum of two temperatures, is oscillating with time but is strictly positive and yields the positive contribution to the covariance. The second term, which is proportional to the difference of two temperatures and thus appears in out-of-equilibrium situations only, is also oscillating and is changing its sign with time. It is also easy to check that the position-velocity covariance is always positive.

Lastly, we determine the position-velocity correlations of the form $\langle x\dot{y} \rangle$ and $\langle y\dot{x} \rangle$. We find

$$\begin{aligned} \langle x\dot{y} \rangle = &- \frac{u(T_1 + T_2)}{4\lambda(1-u^2)} + \frac{(T_1 + T_2)}{8} \left(\frac{\cos(2\Omega_- t)}{\Omega_-^2} - \frac{\cos(2\Omega_+ t)}{\Omega_+^2} \right) \\ &+ \frac{(T_2 - T_1)}{2\lambda u} \left[1 - \cos(\Omega_- t)\cos(\Omega_+ t) - \frac{\sin(\Omega_- t)\sin(\Omega_+ t)}{\sqrt{1-u^2}} \right], \end{aligned} \tag{27}$$

and $\langle y\dot{x} \rangle$ is obtained by switching $T_1 \leftrightarrow T_2$ in Eq.(27).

Equations (27) show that the correlation function between the either position and the velocity of the other component is a bounded oscillating function of time which attains

both negative and positive values at different time moments. These moments vanish, as they should, when either $\lambda \to 0$ or when $u \to 0$.

Together with the expressions for other the moments presented above they determine completely the joint probability density P_t and the characteristic function Φ_t in Eqs. (10) and (9).

4 Two-Time Correlations

To get some additional insight into the time evolution of the processes under study, say of $x(t)$, consider the two-time covariance $\langle x(t)x(t_1)\rangle$. Recall that the analogous covariance of standard Brownian motion is $\langle x(t)x(t_1)\rangle = 2D\min(t_1, t)$ (e.g., $\langle x(t)x(t_1)\rangle = 2Dt_1$ for $t_1 \le t$) with D being the diffusion coefficient. Using Eqs. (14) and performing some straightforward calculations, we find that in our case the covariance function for $t \ge t_1$ is

$$\begin{aligned}\langle x(t)x(t_1)\rangle = {} & \frac{(T_1+T_2)}{4}\, t_1 \left(\frac{\cos(\Omega_+(t-t_1))}{\Omega_+^2} + \frac{\cos(\Omega_-(t-t_1))}{\Omega_-^2}\right) \\ & + \frac{(T_1+T_2)}{4}\left(\frac{\sin(\Omega_+ t_1)\cos(\Omega_+ t)}{\Omega_+^3} + \frac{\sin(\Omega_- t_1)\cos(\Omega_- t)}{\Omega_-^3}\right) \\ & - \frac{(T_1-T_2)}{4u\lambda}\left[\Big(\cos(\Omega_+ t_1) - \cos(\Omega_- t_1)\Big)\left(\frac{\sin(\Omega_+ t)}{\Omega_+} + \frac{\sin(\Omega_- t)}{\Omega_-}\right)\right. \\ & \left. + \Big(\cos(\Omega_+ t) + \cos(\Omega_- t)\Big)\left(\frac{\sin(\Omega_- t_1)}{\Omega_-} - \frac{\sin(\Omega_+ t)}{\Omega_+}\right)\right]\end{aligned} \tag{28}$$

Viewing t_1 as a parameter and t as a variable, we observe that for sufficiently large t_1 (but $t \ge t_1$), the dominant contribution comes from the terms in the first line of the r.h.s. of Eq. (28), while the terms in the second and the third lines show a purely oscillatory behavior and are bounded function of both t and t_1. The amplitude of the dominant terms is proportional to the sum of the temperatures and to t_1, (similarly to the standard Brownian motion). In contrast to the Brownian motion, the amplitude is multiplied by a function of $t - t_1$, which exhibits irregular oscillations. The covariance function is depicted in Fig. 2 as a function of t for two values of t_1 and two values of the temperatures.

5 Position-Velocity Probability Densities

From the joint probability density P_t in Eq. (10) or the characteristic function Φ_t, Eq. (9), together with the exact expressions for the moments and the mixed moments of position and velocity derived in Sect. 3, we can readily calculate the marginal position-velocity distributions $P_t(x, \dot{x})$ and $P_t(y, \dot{y})$. Performing the corresponding Gaussian integrations, we find

$$P_t(x,\dot{x}) = \frac{1}{2\pi\sqrt{\langle x^2\rangle\langle \dot{x}^2\rangle - \langle x\dot{x}\rangle^2}} \exp\left(-\frac{\langle \dot{x}^2\rangle x^2 - 2\langle x\dot{x}\rangle x\dot{x} + \langle x^2\rangle \dot{x}^2}{2\left(\langle x^2\rangle\langle \dot{x}^2\rangle - \langle x\dot{x}\rangle^2\right)}\right), \tag{29}$$

and

$$P_t(y,\dot{y}) = \frac{1}{2\pi\sqrt{\langle y^2\rangle\langle \dot{y}^2\rangle - \langle y\dot{y}\rangle^2}} \exp\left(-\frac{\langle \dot{y}^2\rangle y^2 - 2\langle y\dot{y}\rangle y\dot{y} + \langle y^2\rangle \dot{y}^2}{2\left(\langle y^2\rangle\langle \dot{y}^2\rangle - \langle y\dot{y}\rangle^2\right)}\right). \tag{30}$$

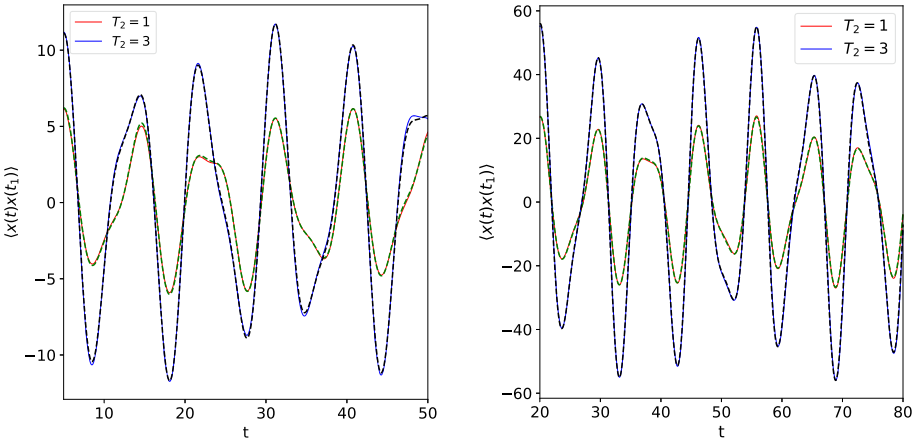

Fig. 2 The covariance function $\langle x(t)x(t_1)\rangle$ versus time t (for $t \geq t_1$) for two values of t_1 and temperatures $T_1 = 1$ and $T_2 = 1, 3$. The coupling parameter $u = 0.5$. Left panel: $t_1 = 5$. Right panel: $t_1 = 20$. Dashed curves correspond to the exact expression, Eq. (28)

Equations (10), (29) and (30) are exponentials of certain quadratic forms of the variables, i.e., are Gaussian as they should be, but the coefficients of the forms are rather complicated functions of the moments. This makes difficult to write them explicitly and we confine ourselves only to their large-time forms

$$P_{t\to\infty}(x,\dot{x}) \simeq \frac{\sqrt{\lambda(1-u^2)}}{\pi(T_1+T_2)t}\exp\Bigg(-\frac{\lambda(1-u^2)x^2}{(T_1+T_2)t}-\frac{\dot{x}^2}{(T_1+T_2)t} + \Bigg[\lambda\left(\frac{\sin^2(\Omega_+ t)}{\Omega_+^2}+\frac{\sin^2(\Omega_- t)}{\Omega_-^2}\right)-\frac{2(T_1-T_2)}{(T_1+T_2)}\sin(\Omega_+ t)\sin(\Omega_- t)\Bigg]\frac{x\,\dot{x}}{(T_1+T_2)t^2}\Bigg), \tag{31}$$

and

$$P_{t\to\infty}(y,\dot{y}) \simeq \frac{\sqrt{\lambda(1-u^2)}}{\pi(T_1+T_2)t}\exp\Bigg(-\frac{\lambda(1-u^2)y^2}{(T_1+T_2)t}-\frac{\dot{y}^2}{(T_1+T_2)t} + \Bigg[\lambda\left(\frac{\sin^2(\Omega_+ t)}{\Omega_+^2}+\frac{\sin^2(\Omega_- t)}{\Omega_-^2}\right)+\frac{2(T_1-T_2)}{(T_1+T_2)}\sin(\Omega_+ t)\sin(\Omega_- t)\Bigg]\frac{y\,\dot{y}}{(T_1+T_2)t^2}\Bigg). \tag{32}$$

We observe that the quadratic terms in the exponents in Eqs. (31) and (32) contain the first inverse power of time, as can be expected from the "diffusive" growth of the second moments of positions and the velocities (see Eqs. (18) and (22)), while the amplitudes of the cross-terms decay at a faster rate proportional to $1/t^2$, showing that the velocities effectively decouple from the positions in the large-t limit. The amplitudes of the cross-terms also contain oscillatory functions that change (aperiodically) their sign with time. We note that this behavior also persists for the total joint probability density $P_t(x, y, \dot{x}, \dot{y})$ in Eq. (10). However, the explicit expression for the corresponding exponent is quite cumbersome even in the limit $t \to \infty$ and we do not present it here. We only mention that, in contrast to the Brownian gyrator model, the limiting forms of $P_t(x, y, \dot{x}, \dot{y})$ and its marginals (Eqs. (31) and (32)) do not exist for the two-dimensional random-acceleration process at $t = \infty$.

6 Gyration Characteristics: Angular Momentum and Angular Velocity

Similarly to the standard analysis of the BGM, we will study now the behavior of the angular momentum $L(t)$, Eq. (12), and the angular velocity $W(t)$, Eq. (13). Recall that the former, which is also called the rotational moment, determines the torque exerted on the particle being at some given instantaneous position, while the latter represents the rate at which the particle at position $\mathbf{r}(t)$ rotates around a fixed origin. Most of available analysis concentrated on the *mean* values of these characteristic properties in the limit $t \to \infty$; both attain finite non-zero values when $T_1 \neq T_2$ and equal zero in equilibrium conditions $T_1 = T_2$ (see, e.g., [10, 14, 16, 17]). On this basis, it was often concluded that the Brownian gyrator is a kind of a "nano-machine" that steadily gyrates around the origin. A recent work [37] has questioned this conclusion by looking on the behavior beyond the mean values. In particular, the probability densities of L and W have been calculated and it was shown that the latter exist only for a time-discretized (with time-step δt) version of the model. In particular, it was also shown that for finite δt the probability density $P_t(L)$ of the angular momentum is always sharply peaked at $L = 0$, and has the exponential tails with different slopes for $T_1 \neq T_2$. This implies that moments of angular momentum of arbitrary order exist, but their values are supported by the tails of the distribution and consequently, do not represent the typical behavior L. Moreover, it was demonstrated that the variance of L is always much larger than the squared first moment, i.e., the "noise" is always greater than the "signal", and diverges in the limit $\delta t \to 0$. More strikingly, the probability density $P_t(W)$ of the angular velocity has algebraic large-W tails of the form $P_t(W) \simeq 1/|W|^3$ such that, in fact, the first moment is the *only* existing moment. This signifies that the spread of the values of angular velocities is infinitely large, although for a large ensemble of "gyrators" there exists some non-zero averaged value of the velocity in out-of-equilibrium conditions. In the limit $\delta t \to 0$, both probability densities converge to uniform distributions with a vanishing amplitude and diverging variance.

We will analyze below the behavior of the moments of the angular momentum and velocity, as well as their probability densities for a random-acceleration process under study along exactly the same lines as it was for the BGM.

6.1 Angular Momentum

According to Eq. (12), the mean value of the angular momentum is given by (recall that we have set $m = 1$)

$$\langle L \rangle = \langle x\dot{y} \rangle - \langle y\dot{x} \rangle, \tag{33}$$

where the terms in the r.h.s. were derived above. Performing some simple calculations, we find that the first moment of the angular momentum obeys for any $t > 0$

$$\langle L \rangle = \frac{(T_2 - T_1)}{\lambda u} \Big(1 - \cos(\Omega_+ t) \cos(\Omega_- t) - \frac{\sin(\Omega_+ t) \sin(\Omega_- t)}{\sqrt{1 - u^2}} \Big). \tag{34}$$

Therefore, the first moment is not identically equal to zero if $T_1 \neq T_2$. Moreover, it is easy to show that the first moment is an odd function of u, and vanishes when $u = 0$. This latter case corresponding to two independent random acceleration processes, such that no angular momentum is expected. However, in contrast to the BGM, $\langle L \rangle$ does not approach a constant value as $t \to \infty$, but rather exhibits irregular oscillations with time and can be positive or negative at different time moments. This means that the torque exerted on the particle changes

the direction at different time moments and the fraction of time that $\langle L\rangle$ has positive values is controlled by the sign of the temperature difference $T_2 - T_1$. For $T_2 - T_1 > 0$, the mean value of the angular moment is predominantly positive, as one can observe from the plot presented on the left panel in Fig. 3.

Consider next the fluctuations of L around its mean value. To this end, it is convenient to use the generalized Wick theorem, according to which if $X = \{X_j\}_{j=1}^m$ is the collection of Gaussian random variables with zero mean and f is a function of X, then we have for $j = 1, 2, \ldots, m$

$$\langle X_j f(X)\rangle = \sum_{k=1}^{m} \langle X_j X_k\rangle \left\langle X_k \frac{\partial f}{\partial X_k}\right\rangle.$$

The theorem follows readily from Eqs. (10) or (9)). This implies, in view of Eq. (12), that

$$\begin{aligned}\left\langle L^2\right\rangle = 2\left\langle x\dot{y}\right\rangle^2 + 2\left\langle \dot{x}y\right\rangle^2 + \left\langle x^2\right\rangle\left\langle \dot{y}^2\right\rangle + \left\langle \dot{x}^2\right\rangle\left\langle y^2\right\rangle \\ - 2\Big(\left\langle xy\right\rangle\left\langle \dot{x}\dot{y}\right\rangle + \left\langle x\dot{y}\right\rangle\left\langle \dot{x}y\right\rangle + \left\langle x\dot{x}\right\rangle\left\langle y\dot{y}\right\rangle \Big).\end{aligned} \tag{35}$$

This and Eq. (33) yield the following expression for the variance of the angular momentum

$$\begin{aligned}\mathrm{Var}\{L\} = \left\langle L^2\right\rangle - \langle L\rangle^2 = \left\langle x\dot{y}\right\rangle^2 + \left\langle \dot{x}y\right\rangle^2 + \left\langle x^2\right\rangle\left\langle \dot{y}^2\right\rangle + \left\langle \dot{x}^2\right\rangle\left\langle y^2\right\rangle \\ - 2\left\langle x\dot{x}\right\rangle\left\langle y\dot{y}\right\rangle - 2\left\langle xy\right\rangle\left\langle \dot{x}\dot{y}\right\rangle,\end{aligned} \tag{36}$$

which is valid for any t. Then, by using the results of Sect. 3, we determine the leading term of the large-t asymptotic form

$$\mathrm{Var}\{L\} \simeq \frac{(T_1 + T_2)^2}{2\lambda(1-u^2)} t^2. \tag{37}$$

It follows from Eq. (34) that $|\langle L\rangle| \le 3|T_2 - T_1|(\lambda u(1-u^2)^{1/2})^{-1}$, and hence, we find that the relative mean square deviation of L (i. e., the coefficient of variation of the corresponding probability density, see, e.g., [64]) obeys the inequality:

$$\frac{(\mathrm{Var}\{L\})^{1/2}}{|\langle L\rangle|} \ge Ct, \;\; C = \frac{(T_1 + T_2)u\sqrt{\lambda}}{|T_1 - T_2|3\sqrt{2}}. \tag{38}$$

Thus, the relative fluctuations of L grow at least linearly in t. Hence, the first moment of the angular momentum does not have much of a physical significance and only indicates some trend in the statistical ensemble.

We conclude that in contrast to many-body physics, where macroscopic observables do not fluctuate and are therefore completely characterized by their mean values, the angular momentum, (as well as the angular velocity, as we will demonstrate below), in our model do not have this property (known as representativeness of averages in statistical physics and self-averaging in disordered media physics). Therefore, in order to obtain complete information about such strongly fluctuating observables, it is necessary to have their complete probability distribution.

This is why we will turn now to the analysis of the probability density of the angular momentum L, Eq. (12). We will begin with the characteristic function of L

$$\Phi_L(\nu) = \langle \exp\left(i\nu\left(x\dot{y} - y\dot{x}\right)\right)\rangle. \tag{39}$$

It is shown Appendix B that

$$\Phi_L(\nu) = \frac{1}{\nu^2\sqrt{\det(M_\nu)}} \tag{40}$$

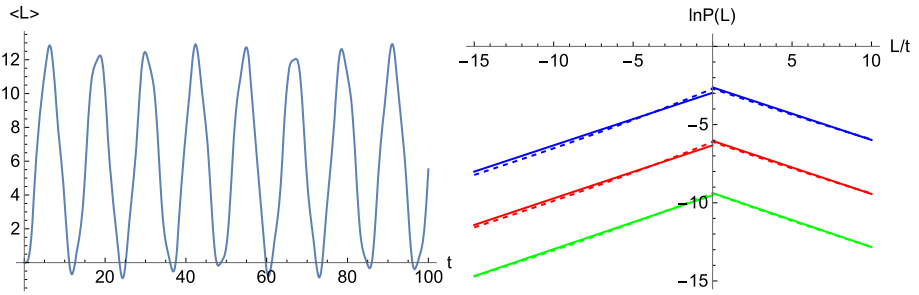

Fig. 3 Angular momentum. Left panel: Mean angular momentum $\langle L\rangle$ versus time for $T_1 = 1, T_2 = 4, u = 1/2$ and $\lambda = 1$. Solid curve depicts the exact result in Eq. (34). Right panel: Logarithm of the probability density $P_t(L)$ as function of scaled variable L/t for $T_1 = 1, T_2 = 4, u = 1/2$ and $\lambda = 1$. Dashed curves correspond to a numerical evaluation of the integral in Eq. (42) for $t = 20$ (blue), $t = 30$ (red) and $t = 40$ (green). Solid curves with the same color code correspond to the asymptotic large-L form in Eq. (43). Note that since all the curves appear too close to each other in the plot, for notational convenience we shifted upwards both blue curves by $+2$, both red curves are shifted downwards by -1 units, and the green curves - by -4 (Color figure online)

where M_ν is a 4×4 matrix

$$M_\nu = M(t) + \frac{1}{\nu}\begin{pmatrix} 0 & -\sigma_y \\ \sigma_y & 0 \end{pmatrix}, \ \sigma_y = \begin{pmatrix} 0 & -i \\ i & 0 \end{pmatrix} \tag{41}$$

and $M(t)$ is given in Eq. (8).

Therefore, the characteristic function $\Phi_L(\nu)$ is the inverse of a square root of a quartic polynomial in ν, whose coefficients can be expressed via the moments of L. In particular, it can be shown that the coefficient in front of ν is $-2i\langle L\rangle$, the coefficient in front of ν^2 is $(\langle L^2\rangle - 3\langle L\rangle^2)$, etc.

Given $\Phi_L(\nu)$, the probability density $P_t(L)$ of L is:

$$P_t(L) = \frac{1}{2\pi}\int_{-\infty}^{\infty} \frac{d\nu}{\nu^2\sqrt{\det(M_\nu)}} \exp(-i\nu L). \tag{42}$$

Despite a relatively simple form of the integrand, the above integral cannot be performed exactly. We hence resort to a numerical evaluation of this integral and its asymptotic analysis in the limit $|L| \to \infty$.

Figure 3 presents the results of a numerical evaluation of $P_t(L)$ in Eq. (42), together with its asymptotic forms (see Eq. (43) below). For convenience, we plot the logarithm of $P_t(L)$ versus a scaled variable L/t. Numerically evaluated $P_t(L)$ is depicted by dashed curves for three values of t: $t = 20$ (blue), $t = 30$ (red) and $t = 40$ (green). We observe that $P_t(L)$ has a cusp at $L = 0$ where it attains the maximal value, similarly to the case of the BGM. Consequently, the first moment of L does not correspond to the typical behavior, when $T_1 \neq T_2$, and is therefore supported by the whole tails of $P_t(L)$ (cf. Equation (38)). For larger L, both right and left tails of the probability density seem to be exponential functions of L/t. In order to verify if this is indeed the case, we turn to Eq. (42) and change the integration variable $\nu \to \nu/t$. Then, we find that the terms with the odd powers of ν in the denominator vanish as $t \to \infty$, and the term ν^4 is relevant only for the short-L behavior. Discarding this

latter term, we get the following large-L asymptotic formula

$$P_t(L) = \frac{\sqrt{\lambda(1-u^2)}}{(T_1+T_2)\,t}\exp\left(-\frac{2\sqrt{\lambda(1-u^2)}}{(T_1+T_2)}\frac{|L|}{t}\right) \times\left(1+\frac{2\sqrt{\lambda(1-u^2)}}{(T_1+T_2)t}\langle L\rangle\,\mathrm{sign}(L)+O\left(\frac{1}{t^2}\right)\right). \tag{43}$$

Hence, the large-L tails of the probability density of the angular momentum are indeed exponential functions of L. Moreover, the left and right tails have the same slope so that $P_t(L)$ for sufficiently large L and t is a symmetric function of L with respect to $L=0$. This is quite different from the behavior of probability density of L observed in the BGM, where the right and left tails have different slopes [37]. The maximal value $P_t(L=0)$ decays as t^{-1} and the slope of the tails tends to zero as $t\to\infty$, which explains why the variance of L grows in proportion to t^2. The asymptotic form of Eq. (43) is depicted in Fig. (3) and we observe that already for $t=40$ it becomes almost indistinguishable from the numerical result.

6.2 Angular Velocity

As in the above case of the angular momentum, it is convenient to use the characteristic function, Eq. (9). In particular, the mean value of the angular velocity (see Eq. (13) with $m=1$) can be conveniently represented as

$$\langle W\rangle = \frac{1}{4\pi}\int_0^\infty\frac{d\xi}{\xi}\int_{-\infty}^{\infty}\int_{-\infty}^{\infty}d\omega_1 d\omega_2\exp\left(-\frac{\omega_1^2+\omega_2^2}{4\xi}\right) \times\left\{\left(-\frac{\partial^2}{\partial\omega_1\partial\omega_4}+\frac{\partial^2}{\partial\omega_2\partial\omega_3}\right)\Phi_t(\boldsymbol{\omega})\right\}\Big|_{\omega_3=\omega_4=0}, \tag{44}$$

where the derivatives with respect to ω-s give the angular momentum, while the integrations over ω_1 and ω_2, and eventually, over ξ, produce the first inverse power of the moment of inertia x^2+y^2. Performing straightforward calculations, we get for any $t>0$ (cf. Equation (34))

$$\langle W\rangle = -\frac{\left(\langle x^2\rangle+\langle y^2\rangle-2\sqrt{\langle x^2\rangle\langle y^2\rangle-\langle xy\rangle^2}\right)}{\left(4\langle xy\rangle^2+\left(\langle x^2\rangle-\langle y^2\rangle\right)^2\right)\sqrt{\langle x^2\rangle\langle y^2\rangle-\langle xy\rangle^2}}\left(\langle xy\rangle\left(\langle y\dot{y}\rangle-\langle x\dot{x}\rangle\right)\right. \left.+\langle y\dot{x}\rangle\left(\langle x^2\rangle+\sqrt{\langle x^2\rangle\langle y^2\rangle-\langle xy\rangle^2}\right)-\langle x\dot{y}\rangle\left(\langle y^2\rangle+\sqrt{\langle x^2\rangle\langle y^2\rangle-\langle xy\rangle^2}\right)\right), \tag{45}$$

The moments entering the above expression are given in Sect. 3.

In the large-t limit, Eq. (45) simplifies considerably to give (cf. Equation (34))

$$\langle W\rangle \simeq \frac{(T_2-T_1)\sqrt{1-u^2}}{(T_1+T_2)ut}\Big(1-\cos(\Omega_+t)\cos(\Omega_-t)\Big). \tag{46}$$

Likewise the first moment of L, Eq. (34), the mean value of W is not identically equal to zero only in "out-of-equilibrium" case where $T_1\neq T_2$; it is also an odd function of u that vanishes for $u=0$. As shown in Fig. 4 (upper panel), $\langle W\rangle$ is an oscillatory function of time whose envelope first rises to some peak value and then decays as the first inverse power of time.

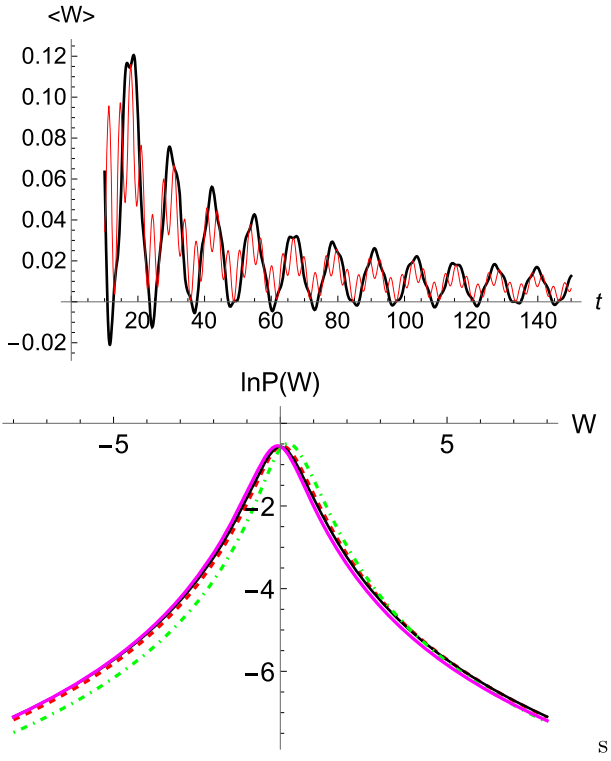

Fig. 4 Angular velocity. Upper panel: Mean angular velocity $\langle W\rangle$ versus time t for $T_1 = 1$, $T_2 = 4$, $u = 1/2$ and $\lambda = 1$. Solid (black) curve depicts the exact result in Eq. (45), while the thin (red) curve presents the large-t asymptotic form in Eq. (46). Lower panel: Logarithm of the probability density $P(W)$ as function of angular velocity for $T_1 = 1$, $T_2 = 4$, $u = 1/2$ and $\lambda = 1$. Dashed green and red curves are the exact results for $t = 5$ and $t = 30$, respectively, obtained by a numerical evaluation of expression (51). Black solid line corresponds to the limiting large-t form in Eq. (54). Solid (magenta) curve depicts the exact result in Eq. (51) for two distinctly different temperatures $T_1 = 50$ and $T_2 = 1$ (Color figure online)

The decay stems from the fact that the particle becomes delocalized and moves away from the origin with time. In addition, similarly to $\langle L\rangle$, $\langle W\rangle$ assumes both positive and negative values. Recall that in the standard BGM the mean angular velocity approaches a constant value in the limit $t \to \infty$ whose sign is defined by the temperature difference.

Consider now the second moment of the angular velocity. This moment can be formally represented as

$$\langle W^2\rangle = \frac{1}{4\pi}\int_0^\infty d\xi \int_{-\infty}^{\infty}\int_{-\infty}^{\infty} d\omega_1 d\omega_2 \exp\left(-\frac{\omega_1^2+\omega_2^2}{4\xi}\right) \times \left\{\left(\frac{\partial^4}{\partial\omega_1^2\partial\omega_4^2} + \frac{\partial^4}{\partial\omega_2^2\partial\omega_3^2} - 2\frac{\partial^4}{\partial\omega_1\partial\omega_2\partial\omega_3\partial\omega_4}\right)\Phi_t(\boldsymbol{\omega})\right\}\Big|_{\omega_3=\omega_4=0}, \tag{47}$$

where the differential operator yields the second power of L, while the integration over ξ gives here the second inverse power of the moment of inertia. Performing differentiations, and then integrating over ω_1 and ω_2, we find some complicated function of ξ. Analyzing the decay of this function in the large-ξ limit, we find that it vanishes as $1/\xi$. This signifies that

the integral over ξ diverges logarithmically at infinity, hence,

$$\langle W^2 \rangle = \infty, \tag{48}$$

which is precisely the behavior encountered previously in the BGM. Consequently, the probability density of the angular velocity has *heavy* power-tails such that the mean angular velocity is the only existing moment.

We turn therefore to the analysis of the probability density of the angular velocity. As in the previous subsection, we consider first the characteristic function of the angular velocity and we find

$$\begin{aligned} \Phi_W(z) &= \left\langle \exp\left(iz \frac{(x\dot{y} - y\dot{x})}{x^2 + y^2} \right) \right\rangle \\ &= \frac{|z|}{2\pi\sqrt{\Delta}} \int_0^{2\pi} d\theta \left(\frac{C_\theta}{A_\theta} \right)^{1/2} K_1\left(\frac{\sqrt{A_\theta C_\theta}}{\Delta} |z| \right) \exp\left(-\frac{i B_\theta z}{2\Delta} \right), \end{aligned} \tag{49}$$

where $K_1(x)$ is the modified Bessel function,

$$\Delta = \langle x^2 \rangle \langle y^2 \rangle - \langle xy \rangle^2, \tag{50}$$

while the coefficients A_θ, B_θ and C_θ are functions of θ and t but do not depend on W. These functions (see Eqs. (C9)), as well as the details of intermediate calculations are presented in Appendix C.

Inverting the Fourier transform, we find next that the probability density function of the angular velocity valid for any t admits the integral representation

$$P_t(W) = \frac{2\Delta^{3/2}}{\pi} \int_0^{2\pi} \frac{C_\theta \, d\theta}{\left(4A_\theta C_\theta + (B_\theta + 2\Delta W)^2\right)^{3/2}} \tag{51}$$

A simple analysis shows that the large-W asymptotic form of P_t is

$$P_t(W) \simeq \frac{\alpha}{|W|^3}, \;\; \alpha = \frac{1}{4\pi\Delta^{3/2}} \int_0^{2\pi} C_\theta \, d\theta. \tag{52}$$

i.e., α depends on time, both temperatures and the parameters characterizing the potential (see Eqs. (C9)). In Fig. 4 we depict the results of a numerical evaluation of the integral in Eq. (51) together with the asymptotic form in Eq. (52) (see below).

Now, we consider the behavior of $P_t(W)$ in Eq. (51) in the limit $t \to \infty$ and W bounded away from zero, which appears to be quite non-trivial. To this end, we observe that in the limit $t \to \infty$ the function B_θ (see Eqs. (C9)) grows linearly with time, i.e., $B_\theta \simeq t\,\Gamma_\theta$, where Γ_θ is a rather complicated function of θ, u, λ and both temperatures, but is independent of time. On the other hand, the asymptotic behavior of the functions

$$\begin{aligned} A_\theta &\simeq \frac{(T_1 + T_2)(1 + u\sin(2\theta))}{2\lambda(1 - u^2)}\, t, \\ C_\theta &\simeq \frac{(T_1 + T_2)^3}{8\lambda^2(1 - u^2)}\, t^3, \\ \Delta &\simeq \frac{(T_1 + T_2)^2}{4\lambda^2(1 - u^2)} t^2, \end{aligned} \tag{53}$$

is given by explicit and fairly compact expressions. Inserting these expressions into Eq. (51), we find that $P_t(W)$ attains the following limiting ($t = \infty$) form, valid for any $W \neq 0$:

$$P_\infty(W) \simeq \frac{\lambda\sqrt{1-u^2}}{8\pi\left(\lambda + W^2\right)^{3/2}} \int_0^\pi \frac{d\theta}{(1+\kappa\sin(\theta))^{3/2}}, \quad \kappa = \frac{\lambda u}{\lambda + W^2}. \tag{54}$$

The integral in Eq. (54) can be expressed through the elliptic integrals. But its large-W asymptotic form follows directly from Eq. (54), (e.g., by expanding the integrand into the Taylor series in powers of κ):

$$P(W) \simeq \frac{\lambda\sqrt{1-u^2}}{8|W|^3}, \; W \to \pm\infty, \tag{55}$$

(cf. Equation (52)).

We observe a certain stabilization effect appearing in a driven system without friction.

Curiously enough, in the limit $t \to \infty$, the amplitude α in Eq. (52) does not depend on the temperatures T_1 and T_2. To verify this rather strange prediction, we also depict by the solid magenta curve in Fig. 4 the result of a numerical evaluation of the expression (51) for two quite different temperatures $T_1 = 50$ and $T_2 = 1$ (note that other curves correspond to $T_1 = 1$ and $T_2 = 4$) at time $t = 30$. We observe that even for this quite moderate value of t, the curve is very close to our prediction in Eq. (55) thereby confirming the temperature-independent form of the long-time limit in Eq. (55). While we are unable to provide simple physical arguments explaining this intriguing behavior, it seems to be quite evident from the mathematical point of view. Indeed, the angular velocity is formally defined as the ratio of the angular momentum and the moment of inertia $I = x^2 + y^2$ (see Eq. (13)) which is formally equal to $2U_{u=0}(t)/\lambda$, where $U_{u=0}(t)$ is the potential energy of the particle at zero value of the coupling parameter u. In the next Section, we determine the large-t asymptotic form of the probability density of $U(t)$, see Eq. (63), and show that the temperatures enter this function only via their sum $T_1 + T_2$. In other words, for $t \to \infty$ and for most of realizations of the process we have $I = (T_1 + T_2)\mathcal{I}$, where $\mathcal{I}$ is a temperature-independent random variable with exponential distribution. In turn, our analysis of the large-t asymptotic form of the probability density of the angular momentum (see Eq. (43)) also shows that the latter incorporates the temperatures only via their sum, suggesting that for the most of the realizations the angular momentum behaves as $L = (T_1 + T_2)\mathcal{L}$ where $\mathcal{L}$ is temperature-independent. In view of this argument, it does not seem surprising that the large-t and large-W asymptotic form of the probability density function of $W = \mathcal{I}/\mathcal{L}$ is independent of the temperatures.

7 Kinetic, Potential and Total Energy

The energy is continuously pumped into the system and, in absence of a dissipation, is therefore increasing with time. Concurrently, since the particle performs a random motion, its energy is a random variable and it seems interesting to study its statistical properties. We consider separately the potential energy $U(t)$, defined in Eq. (1), kinetic energy

$$K(t) = \left(\dot{x}^2 + \dot{y}^2\right)/2, \tag{56}$$

and the total energy $E(t) = U(t) + K(t)$.

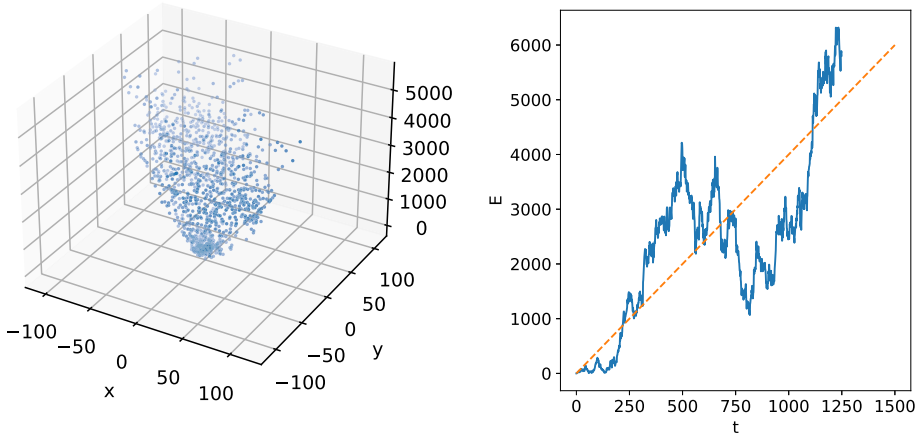

Fig. 5 The total energy $E(t)$ of the particle for a given realization of noises, $u = 1/2$, $T_1 = 1$ and $T_2 = 2$. Left panel: The spread of $E(t)$ for consecutive positions of the particle on the (x, y)-plane. Right panel: $E(t)$ as function of time for a given trajectory of the particle (blue noisy curve). The dashed line depicts the mean total energy $\langle E(t)\rangle$ in Eq. (58) (Color figure online)

Using the expressions for the moments of positions and velocities, derived in Sect. 3, we readily find that the first moments of the energies obey

$$\begin{aligned}\langle U(t)\rangle &= \frac{(T_1+T_2)}{2}t - \frac{(T_1+T_2)}{8}\left(\frac{\sin(2\Omega_+ t)}{\Omega_+} + \frac{\sin(2\Omega_- t)}{\Omega_-}\right),\\ \langle K(t)\rangle &= \frac{(T_1+T_2)}{2}t + \frac{(T_1+T_2)}{8}\left(\frac{\sin(2\Omega_+ t)}{\Omega_+} + \frac{\sin(2\Omega_- t)}{\Omega_-}\right),\end{aligned} \tag{57}$$

and therefore,

$$\langle E(t)\rangle = (T_1+T_2)\,t. \tag{58}$$

We note that the mean potential and the kinetic energies are both linearly growing with time, in the leading order, and also contain some sub-dominant oscillatory terms. The prefactor in the dominant linear dependence on time is just the sum of the temperatures, as it should be, and is independent of the strength λ of the potential and of the coupling parameter u. In turn, the mean total energy is simply a monotonically growing function of time, because the sub-dominant oscillatory terms cancel each other.

In Fig. 5 we depict the total energy of the particle for a single realization of the particle's trajectory. We observe significant fluctuations: indeed, the spread of realization-dependent values around the mean one appears to be very large. Therefore, to fully quantify the temporal evolution of the energies it is necessary to go beyond the mean values and to determine the full probability density functions of the energies. This can be done by standard means, i.e., by evaluating first the respective characteristic functions and then inverting the corresponding Laplace transforms. In doing so and omitting the intermediate calculations, we find that the probability densities $P_t(U)$ and $P_t(K)$ of the potential and of the kinetic energies are

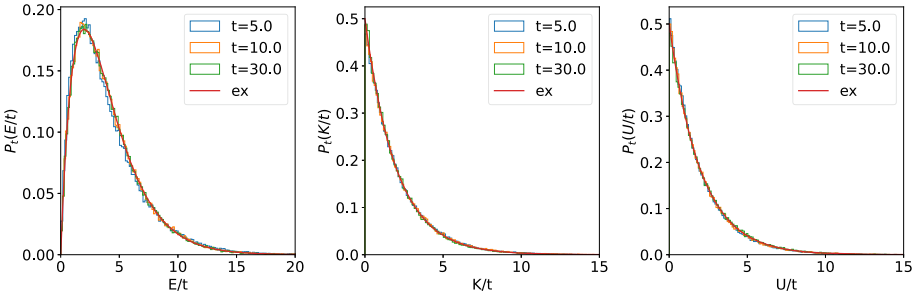

Fig. 6 Probability densities of the energies. Solid (red) curves depict the asymptotic forms in Eq. (63), while the noisy curves represents the probability density functions deduced from numerical simulations (Color figure online)

$$
\begin{aligned}
P_t(U) &= \frac{1}{\lambda\sqrt{(1-u^2)\Delta}} \exp\left(-\frac{\langle U\rangle}{(1-u^2)\Delta\lambda^2}U\right) I_0\left(b\,U\right), \\
b &= \frac{\sqrt{\langle U\rangle^2 - (1-u^2)\Delta\lambda^2}}{(1-u^2)\Delta\lambda^2}, \quad \Delta = \langle x^2\rangle\langle y^2\rangle - \langle xy\rangle^2, \\
P_t(K) &= \frac{1}{\sqrt{\Delta'}} \exp\left(-\frac{\langle K\rangle}{\Delta'}K\right) I_0\left(\frac{\sqrt{\langle K\rangle^2 - \Delta'}}{\Delta'}K\right), \quad \Delta' = \langle \dot{x}^2\rangle\langle \dot{y}^2\rangle - \langle \dot{x}\,\dot{y}\rangle^2
\end{aligned}
\tag{59}
$$

where $I_0(z)$ is the modified Bessel function, while $\langle U\rangle$ and $\langle K\rangle$ are defined in Eqs. (57). In turn, the probability density of the total energy cannot be obtained in a closed form but rather in form of the inverse Laplace transform of the inverse of a square root of a fourth-order polynomial of the Laplace parameter s:

$$
P_t(E) = \mathcal{L}^{-1}_{s,E}\left\{\frac{1}{\sqrt{\left(1+2\langle K\rangle s + \Delta' s^2\right)\left(1+2\langle U\rangle s + (1-u^2)\lambda^2\Delta\, s^2\right)}}\right\}. \tag{60}
$$

To quantify fluctuations of the energies, we determine their variances. This can be done directly by integrating the probability density functions in Eqs. (59), and by differentiating the kernel function in Eq. (60) with respect to s and then setting $s = 0$. This gives the following exact expressions

$$
\begin{aligned}
\mathrm{Var}\{U\} &= 2\langle U\rangle^2 - (1-u^2)\Delta\lambda^2, \\
\mathrm{Var}\{K\} &= 2\langle K\rangle^2 - \Delta', \\
\mathrm{Var}\{E\} &= 2\langle U\rangle^2 + 2\langle K\rangle^2 - \Delta' - (1-u^2)\Delta\lambda^2.
\end{aligned}
\tag{61}
$$

In particular, we find that the coefficients of variation of the probability density of the energies admits the limits

$$
\lim_{t\to\infty}\frac{\sqrt{\mathrm{Var}\{U\}}}{\langle U\rangle} = \lim_{t\to\infty}\frac{\sqrt{\mathrm{Var}\{K\}}}{\langle K\rangle} = \lim_{t\to\infty}\frac{\sqrt{\mathrm{Var}\{E\}}}{\langle E\rangle} = 1, \tag{62}
$$

signifying that fluctuations are exactly of the same order of magnitude as the mean values themselves. Consequently, the corresponding probability densities are effectively broad (see, e.g., [64]) and the mean values do not characterize the behavior of energies adequately well.

Lastly, we analyze the large-energy tails of the probability densities (59) and (60). It is quite straightforward for the potential and kinetic energies whose distributions are given by

simple explicit forms in Eqs. (59) and only slightly more involved for the total energy whose probability density is given implicitly, in form of the inverse Laplace transform in Eq. (60). We proceed here exactly in the same way as in Sect. 6 for the evaluation of the limiting form of the probability density of the angular moment. That being, we turn to the variable E/t and consider the large-t behavior of the coefficients of the fourth-order polynomial in s. In doing so, we eventually find that all three probability densities have simple exponential tails of the form:

$$\begin{aligned} P_{t\to\infty}(U) &\simeq \frac{2}{(T_1+T_2)t}\exp\left(-\frac{2U}{(T_1+T_2)t}\right), \\ P_{t\to\infty}(K) &\simeq \frac{2}{(T_1+T_2)t}\exp\left(-\frac{2K}{(T_1+T_2)t}\right), \\ P_{t\to\infty}(E) &\simeq \frac{4E}{(T_1+T_2)^2t^2}\exp\left(-\frac{2E}{(T_1+T_2)t}\right). \end{aligned} \tag{63}$$

The probability densities in Eqs. (63) are depicted in Fig. 6 together with the corresponding forms obtained in the numerical simulations. We observe an excellent agreement between our theoretical predictions and numerics even for quite modest times. Lastly, we note that, in contrast to the probability densities of the kinetic and the potential energies which are monotonically decreasing functions, the probability density function of the total energy has a maximum, which determines the most probable total energy, i.e., the value that should be observed for the majority of realizations of the process,

$$E_{\rm mp} = \frac{(T_1+T_2)t}{2}, \tag{64}$$

which appears to be two times smaller than the mean total energy, Eq. (58). This again signifies that fluctuations are very important.

8 Conclusions

To conclude, we studied here the dynamics of a particle which moves randomly on a plane and the position components are defined as two linearly coupled random-acceleration processes evolving in a parabolic confining potential. Each position component is subject to its own independent Gaussian noise with the amplitude (temperature) is, in general, not equal to that of the noise acting on the other component. Our analysis was motivated, in part, by recent interesting observations made in [16, 17] for a finite-mass Brownian gyrator model in the non-equilibrium steady-state attained in the limit $t \to \infty$. Here we concentrated rather on the large-_ but finite-time behavior in a somewhat simplified system in which the damping (and hence, the dissipation) is set equal to zero. Therefore, apart of being of an interest in its own right, our model and the results can be considered as describing the temporal evolution of a finite-mass gyrator at transient stages, if the mass is sufficiently large.

In addition to the standard characteristics, such as, e.g., the moments and the mixed moments, the two-time correlations and the position-velocity probability density function, we also determined the characteristics of the rotational motion - the angular momentum and the angular velocity. We have shown that in case when the amplitudes of noises acting on the components are not equal, the angular momentum and the angular velocity have non-zero mean values. However, unlike it happens for the Brownian gyrator for which these properties approach constant values, for the model under study they show irregular oscillations with

time, meaning that the torque exerted on the particle aperiodically changes its sign at different time moments and the particle is prompted to rotate clockwise and then counter-clockwise.

Looking on these random variables from a broader perspective, we found the full probability densities of the angular momentum L and of the angular velocity W. We showed that the former has simple exponential large-L tails for any large but fixed time, and hence, all moments are finite at a finite t. These asymptotic tails are symmetric with respect to the sign of L and hence, a non-zero value of the first moment stems from the asymmetry of the probability density at small values of L. In the limit $t \to \infty$, this latter probability density function converges to a uniform distribution with a diverging variance, which signifies that fluctuations become very significant. In turn, we found that the probability density of the angular velocity possesses heavy power-law tails $1/|W|^3$ and hence, the mean angular velocity is the only existing moment. Therefore, fluctuations of the angular velocity destroy any systematic rotational motion.

We note parenthetically that the heavy tails of the form $1/|W|^3$ are exactly the same that were previously found for the standard Brownian gyrator [37]. Given that the dynamics in both models is quite different, it is tempting to believe that such tails is a generic feature resulted from the Gaussian noise acting on the particle. In this regard, it seems interesting to verify whether this feature will remain valid also for a more general model of a finite-mass Brownian gyrator.

Acknowledgements L.P. is grateful to the Ecole Normale Superieure (Paris, France) and the Institut des Hautes Etudes Scientifiques (Bures sur Yvette, France) for the stay during which part of this work has been carried out.

Data Availability Data sharing not applicable to this article as no datasets were generated or analyzed during the current study.

Declarations

Conflict of interest The authors declare that they have no conflicts of interest.

Appendix A The Proof of Invertibility of $M(t)$

It is convenient to rewrite the system (4) – (5) of two equation of second order for $x(t)$ and $y(t)$ as the system of four equation of first order for $X(t)$ of (6):

$$\dot{\mathbf{X}}(t) = A\mathbf{X}(t) + B\boldsymbol{\xi}(t), \ \mathbf{X}(0) = 0, \tag{A1}$$

where

$$A = \begin{pmatrix} \mathbf{0} & \mathbf{1} \\ -\mathbf{a} & \mathbf{0} \end{pmatrix}, \ B = \begin{pmatrix} \mathbf{0} & \mathbf{0} \\ \mathbf{0} & \mathbf{1} \end{pmatrix}, \ \boldsymbol{\xi}(t) = \begin{pmatrix} 0 \\ \boldsymbol{\xi}^{(2)}(t) \end{pmatrix},$$

i.e., A and B are 4×4 matrices written as 2×2 matrices with 2×2 blocks and ξ is 4×1 vector written as 2×1 vector with 2×1 components

$$\mathbf{0} = \begin{pmatrix} 0 & 0 \\ 0 & 0 \end{pmatrix}, \ \mathbf{1} = \begin{pmatrix} 1 & 0 \\ 0 & 1 \end{pmatrix}, \ \mathbf{a} = \lambda \begin{pmatrix} 1 & u \\ u & 1 \end{pmatrix}, \ \boldsymbol{\xi}^{(2)}(t) = \begin{pmatrix} \xi_1(t) \\ \xi_2(t) \end{pmatrix}.$$

Then

$$\mathbf{X}(t) = \int_0^t e^{A(t-s)} B\boldsymbol{\xi}(s) ds,$$

and (3) and (8) yield

$$M(t) = \int_0^t e^{As} \mathcal{B} e^{A^T s} ds, \tag{A2}$$

where

$$\mathcal{B} = \begin{pmatrix} \mathbf{0} & \mathbf{0} \\ \mathbf{0} & \mathbf{b} \end{pmatrix}, \ \mathbf{b} = \begin{pmatrix} 2T_1/m^2 & 0 \\ 0 & 2T_2/m^2 \end{pmatrix}.$$

We have

$$A^2 = -\begin{pmatrix} \mathbf{a} & \mathbf{0} \\ \mathbf{0} & \mathbf{a} \end{pmatrix} = -\begin{pmatrix} \mathbf{a}^{1/2} & \mathbf{0} \\ \mathbf{0} & \mathbf{a}^{1/2} \end{pmatrix}^2 = -\mathcal{A}^2,$$

hence, $e^{As} = \cos \mathcal{A}s + A(\sin \mathcal{A}s)/\mathcal{A}$. This, the spectral expansion of

$$\mathbf{a} = \lambda(1+u)|\psi_+\rangle\langle\psi_+| + \lambda(1-u)|\psi_-\rangle\langle\psi_-|, \ |\psi_+\rangle = 2^{-1/2}\begin{pmatrix} 1 \\ \pm 1 \end{pmatrix}.$$

and a simple but somewhat tedious algebra allow us to show that $M(t)$ is invertible for any $t > 0$.

Appendix B Characteristic Function of the Angular Momentum

We start with the formal definition

$$\begin{aligned} \Phi_L(\nu) &= \langle \exp\left(i\nu\,(x\dot{y} - y\dot{x})\right)\rangle \\ &= \int_{-\infty}^{\infty}\int_{-\infty}^{\infty}\int_{-\infty}^{\infty}\int_{-\infty}^{\infty} dx\,dy\,d\dot{x}\,d\dot{y}\,\exp\left(i\nu\,(x\dot{y} - y\dot{x})\right)\,\mathcal{P}_t\,(x,y,\dot{x},\dot{y})\,. \end{aligned} \tag{B3}$$

Expressing the joint position-velocity probability density through its characteristic function, we have that the characteristic function of the angular momentum can be formally written as

$$\begin{aligned} \Phi_L(\nu) &= \frac{1}{(2\pi)^4}\int_{-\infty}^{\infty}\int_{-\infty}^{\infty}\int_{-\infty}^{\infty}\int_{-\infty}^{\infty} d\omega_1\,d\omega_2\,d\omega_3\,d\omega_4\,\Phi_t(\boldsymbol{\omega}) \\ &\quad\times\int_{-\infty}^{\infty}\int_{-\infty}^{\infty}\int_{-\infty}^{\infty}\int_{-\infty}^{\infty} dx\,dy\,d\dot{x}\,d\dot{y}\,\exp\left(i\nu\,(x\dot{y} - y\dot{x})\right. \\ &\quad\left. -i\omega_1 x - i\omega_2 y - i\omega_3\dot{x} - i\omega_4\dot{y}\right) \\ &= \frac{1}{(2\pi)^2}\int_{-\infty}^{\infty}\int_{-\infty}^{\infty}\int_{-\infty}^{\infty}\int_{-\infty}^{\infty} d\omega_1\,d\omega_2\,d\omega_3\,d\omega_4\,\Phi_t(\boldsymbol{\omega}) \\ &\quad\times\int_{-\infty}^{\infty}\int_{-\infty}^{\infty} d\dot{x}\,d\dot{y}\,\exp \\ &\quad\left(-i\omega_3\dot{x} - i\omega_4\dot{y}\right)\delta\left(\nu\dot{y} - \omega_1\right)\,\delta\left(\nu\dot{x} + \omega_2\right). \end{aligned} \tag{B4}$$

Performing next the integrals over $\dot{x}$ and $\dot{y}$, we get

$$\Phi_L(\nu) = \frac{1}{(2\pi)^2\nu^2}\int_{-\infty}^{\infty}\int_{-\infty}^{\infty}\int_{-\infty}^{\infty}\int_{-\infty}^{\infty} d\omega_1\,d\omega_2\,d\omega_3\,d\omega_4\,\Phi_t(\boldsymbol{\omega})\exp\left(i\,\frac{\omega_2\omega_3}{\nu} - i\,\frac{\omega_1\omega_4}{\nu}\right). \tag{B5}$$

Performing Gaussian integrals yields the exact expression in Eqs. (40) and (41).

Appendix C Characteristic Function of the Angular Velocity

We start with the formal definition

$$\begin{aligned}\Phi_W(z) &= \left\langle \exp\left(iz\frac{(x\dot{y}-y\dot{x})}{x^2+y^2}\right)\right\rangle \\ &= \int_{-\infty}^{\infty}\int_{-\infty}^{\infty}\int_{-\infty}^{\infty}\int_{-\infty}^{\infty} dx\,dy\,d\dot{x}\,d\dot{y}\,\exp\left(iz\frac{(x\dot{y}-y\dot{x})}{x^2+y^2}\right)\mathcal{P}_t\,(x,y,\dot{x},\dot{y})\,.\end{aligned} \tag{C6}$$

Expressing again the joint position-velocity probability density through its characteristic function, we find that the characteristic function of the angular velocity can be formally written as

$$\begin{aligned}\Phi_W(z) &= \frac{1}{(2\pi)^4}\int_{-\infty}^{\infty}\int_{-\infty}^{\infty}\int_{-\infty}^{\infty}\int_{-\infty}^{\infty} d\omega_1\,d\omega_2\,d\omega_3\,d\omega_4\,\Phi_t(\boldsymbol{\omega}) \\ &\quad\times\int_{-\infty}^{\infty}\int_{-\infty}^{\infty}\int_{-\infty}^{\infty}\int_{-\infty}^{\infty} dx\,dy\,d\dot{x}\,d\dot{y}\,\exp \\ &\quad\left(iz\frac{(x\dot{y}-y\dot{x})}{x^2+y^2} - i\omega_1 x - i\omega_2 y - i\omega_3\dot{x} - i\omega_4\dot{y}\right) \\ &= \frac{1}{(2\pi)^2}\int_{-\infty}^{\infty}\int_{-\infty}^{\infty}\int_{-\infty}^{\infty}\int_{-\infty}^{\infty} d\omega_1\,d\omega_2\,d\omega_3\,d\omega_4\,\Phi_t(\boldsymbol{\omega}) \\ &\quad\times\int_{-\infty}^{\infty}\int_{-\infty}^{\infty} dx\,dy\,\exp\left(-i\omega_1 x - i\omega_2 y\right)\delta\left(\frac{zy}{x^2+y^2}+\omega_3\right)\delta\left(\frac{zx}{x^2+y^2}-\omega_4\right).\end{aligned} \tag{C7}$$

Performing first the integrals over ω_3 and ω_4, then over ω_1 and ω_2, we change the integration variables x and y for polar coordinates $x=\rho\cos(\theta)$ and $y=\rho\sin(\theta)$ to get

$$\begin{aligned}\Phi_W(z) &= \frac{1}{2\pi\sqrt{\langle x^2\rangle\langle y^2\rangle-\langle xy\rangle^2}}\int_0^{2\pi} d\theta\int_0^{\infty}\rho\,d\rho\,\exp \\ &\quad\left(-\frac{A_\theta\rho^2+iB_\theta z+C_\theta z^2/\rho^2}{2\left(\langle x^2\rangle\langle y^2\rangle-\langle xy\rangle^2\right)}\right),\end{aligned} \tag{C8}$$

where the functions A_θ, B_θ and C_θ are given explicitly by

$$\begin{aligned}A_\theta &= \langle x^2\rangle\sin^2(\theta)+\langle y^2\rangle\cos^2(\theta)-\langle xy\rangle\sin(2\theta) \\ B_\theta &= 2\left(\langle xy\rangle\langle y\dot{y}\rangle-\langle y^2\rangle\langle x\dot{y}\rangle\right)\cos^2(\theta)-2\left(\langle xy\rangle\langle x\dot{x}\rangle-\langle x^2\rangle\langle y\dot{x}\rangle\right)\sin^2(\theta) \\ &\quad+\left(\langle xy\rangle\langle x\dot{y}\rangle-\langle xy\rangle\langle y\dot{x}\rangle+\langle y^2\rangle\langle x\dot{x}\rangle-\langle x^2\rangle\langle y\dot{y}\rangle\right)\sin(2\theta) \\ C_\theta &= \frac{1}{2}\Big[\left(\langle x^2\rangle\langle y^2\rangle-\langle xy\rangle^2\right)\left(\langle\dot{x}^2\rangle+\langle\dot{y}^2\rangle\right)-2\Big(\langle y^2\rangle\langle x\dot{y}\rangle^2+\langle x^2\rangle\langle y\dot{y}\rangle^2 \\ &\quad-2\langle xy\rangle\langle x\dot{y}\rangle\langle y\dot{y}\rangle\Big)\cos^2(\theta)-2\Big(\langle x^2\rangle\langle y\dot{x}\rangle^2+\langle y^2\rangle\langle x\dot{x}\rangle^2-2\langle xy\rangle\langle x\dot{x}\rangle\langle y\dot{x}\rangle\Big)\sin^2(\theta) \\ &\quad-\left(\langle x^2\rangle\langle y^2\rangle-\langle xy\rangle^2\right)\left(\langle\dot{x}^2\rangle-\langle\dot{y}^2\rangle\right)\cos(2\theta)+2\Big(\langle xy\rangle^2\langle\dot{x}\dot{y}\rangle+\langle x^2\rangle\langle y\dot{x}\rangle\langle y\dot{y}\rangle \\ &\quad+\langle y^2\rangle\langle x\dot{x}\rangle\langle x\dot{y}\rangle-\langle xy\rangle\langle x\dot{y}\rangle\langle y\dot{x}\rangle-\langle xy\rangle\langle x\dot{x}\rangle\langle y\dot{y}\rangle-\langle x^2\rangle\langle y^2\rangle\langle\dot{x}\dot{y}\rangle\Big)\sin(2\theta)\Big].\end{aligned} \tag{C9}$$

Performing in Eq. (C8) the integration over ρ, we arrive at our Eq. (49).

References

1. Bodineau, T., Derrida, B.: Current fluctuations in nonequilibrium diffusive systems: An additivity principle. Phys. Rev. Lett. **92**(18), 180601 (2004). https://doi.org/10.1103/PhysRevLett.92.180601
2. Visco, P.: Work fluctuations for a brownian particle between two thermostats. J. Stat. Mech. Theo. Exp. **2006**(06), 06006 (2006). https://doi.org/10.1088/1742-5468/2006/06/P06006
3. Fogedby, H.C., Imparato, A.: A bound particle coupled to two thermostats. J. Stat. Mech. Theo. Exp. **2011**(05), 05015 (2011). https://doi.org/10.1088/1742-5468/2011/05/P05015
4. Evans, D.J., Searles, D.J.: The fluctuation theorem. Adv. Phys. **51**, 1529–1585 (2002). https://doi.org/10.1080/00018730210155133
5. Marini, U.B.M., Puglisi, A., Rondoni, L., Vulpiani, A.: Fluctuation-dissipation: response theory in statistical physics. Phys. Rep. **461**, 111–195 (2008). https://doi.org/10.1016/j.physrep.2008.02.002
6. Rondoni, L., Mejía-Monasterio, C.: Fluctuations in nonequilibrium statistical mechanics: models, mathematical theory, physical mechanisms. Nonlinearity **20**(10), 1–37 (2007). https://doi.org/10.1088/0951-7715/20/10/r01
7. Seifert, U.: Stochastic thermodynamics, fluctuation theorems and molecular machines. Rep. Prog. Phys. **75**, 126001 (2012). https://doi.org/10.1088/0034-4885/75/12/126001
8. Wang, M.C., Uhlenbeck, G.E.: On the theory of the brownian motion ii. Rev. Mod. Phys. **17**, 323–342 (1945). https://doi.org/10.1103/RevModPhys.17.323
9. Exartier, R., Peliti, L.: A simple system with two temperatures. Phys. Lett. A **261**(1), 94–97 (1999). https://doi.org/10.1016/S0375-9601(99)00606-4
10. Filliger, R., Reimann, P.: Brownian gyrator: A minimal heat engine on the nanoscale. Phys. Rev. Lett. **99**, 230602 (2007). https://doi.org/10.1103/PhysRevLett.99.230602
11. Ciliberto, S., Imparato, A., Naert, A., Tanase, M.: Heat flux and entropy produced by thermal fluctuations. Phys. Rev. Lett. **110**, 180601 (2013). https://doi.org/10.1103/PhysRevLett.110.180601
12. Ciliberto, S., Imparato, A., Naert, A., Tanase, A.: Statistical properties of the energy exchanged between two heat baths coupled by thermal fluctuations. J. Stat. Mech. **2013**(12), 12014 (2013). https://doi.org/10.1088/1742-5468/2013/12/P12014
13. Bérut, A., Petrosyan, A., Ciliberto, S.: Energy flow between two hydrodynamically coupled particles kept at different effective temperatures. Europhys. Lett. **107**(6), 60004 (2014). https://doi.org/10.1209/0295-5075/107/60004
14. Dotsenko, V., Maciołek, A., Vasilyev, O., Oshanin, G.: Two-temperature langevin dynamics in a parabolic potential. Phys. Rev. E **87**, 062130 (2013). https://doi.org/10.1103/PhysRevE.87.062130
15. Fogedby, H.C., Imparato, A.: A minimal model of an autonomous thermal motor. Europhys. Lett. **119**(5), 50007 (2017). https://doi.org/10.1209/0295-5075/119/50007
16. Mancois, V., Marcos, B., Viot, P., Wilkowski, D.: Two-temperature brownian dynamics of a particle in a confining potential. Phys. Rev. E **97**, 052121 (2018). https://doi.org/10.1103/PhysRevE.97.052121
17. Bae, Y., Lee, S., Kim, J., Jeong, H.: Inertial effects on the brownian gyrator. Phys. Rev. E **103**, 032148 (2021). https://doi.org/10.1103/PhysRevE.103.032148
18. Alberici, D., Macris, N., Mingione, E.: On the convergence to the non-equilibrium steady state of a Langevin dynamics with widely separated time scales and different temperatures. Ann. Henri Poincaré (2024). https://doi.org/10.1007/s00023-023-01392-0
19. Siches, J.V., Miangolarra, O.M., Taghvaei, A., Georgiou, T.T.: Inertialess gyrating engines. PNAS Nexus **1**, 1–9 (2022). https://doi.org/10.1093/pnasnexus/pgac251
20. Baldassarri, A., Puglisi, A., Sesta, L.: Engineered swift equilibration of a brownian gyrator. Phys. Rev. E **102**, 030105 (2020). https://doi.org/10.1103/PhysRevE.102.030105
21. Nascimento, S.E., Morgado, W.A.M.: Stationary properties of a non-markovian brownian gyrator. J. Stat. Mech. Theo. Exp. **2021**(1), 013301 (2021). https://doi.org/10.1088/1742-5468/abd027
22. Squarcini, A., Solon, A., Viot, P., Oshanin, G.: Fractional brownian gyrator. J. Phys. A: Math. Theo. **55**(48), 485001 (2022). https://doi.org/10.1088/1751-8121/aca4aa
23. Crisanti, A., Puglisi, A., Villamaina, D.: Nonequilibrium and information: The role of cross correlations. Phys. Rev. E **85**, 061127 (2012). https://doi.org/10.1103/PhysRevE.85.061127
24. Mazzolo, A., Monthus, C.: Nonequilibrium diffusion processes via non-hermitian electromagnetic quantum mechanics with application to the statistics of entropy production in the brownian gyrator. Phys. Rev. E **107**, 014101 (2023). https://doi.org/10.1103/PhysRevE.107.014101
25. Movilla Miangolarra, O., Taghvaei, A., Fu, R., Chen, Y., Georgiou, T.T.: Energy harvesting from anisotropic fluctuations. Phys. Rev. E **104**, 044101 (2021). https://doi.org/10.1103/PhysRevE.104.044101
26. Miangolarra, O.M., Taghvaei, A., Chen, Y., Georgiou, T.T.: Thermodynamic engine powered by anisotropic fluctuations. Phys. Rev. Res. **4**, 023218 (2022). https://doi.org/10.1103/PhysRevResearch.4.023218

27. Chang, H., Lee, C.-L., Lai, P.-Y., Chen, Y.-F.: Autonomous brownian gyrators: A study on gyrating characteristics. Phys. Rev. E **103**, 022128 (2021). https://doi.org/10.1103/PhysRevE.103.022128
28. Dutta, S., Saha, A.: Microscopic gyration with dissipative coupling. https://doi.org/10.48550/arXiv.2308.02085
29. Squarcini, A., Marinari, E., Oshanin, G., Peliti, L., Rondoni, L.: Frequency-frequency correlations of single-trajectory spectral densities of gaussian processes. New J. Phys. **24**(9), 093031 (2022). https://doi.org/10.1088/1367-2630/ac8f65
30. Cerasoli, S., Ciliberto, S., Marinari, E., Oshanin, G., Peliti, L., Rondoni, L.: Spectral fingerprints of nonequilibrium dynamics: The case of a brownian gyrator. Phys. Rev. E **106**, 014137 (2022). https://doi.org/10.1103/PhysRevE.106.014137
31. Dotsenko, V.S., Viot, P., Imparato, A., Oshanin, G.: Cooperative dynamics in two-component out-of-equilibrium systems: molecular 'spinning tops'. J. Stat. Mech. Theo. Exp. **2022**(12), 123211 (2022). https://doi.org/10.1088/1742-5468/aca900
32. Dotsenko, V.S., Imparato, A., Viot, P., Oshanin, G.: Out-of-equilibrium dynamics of two interacting optically-trapped particles. SciPost Phys. Core **6**, 056 (2023). https://scipost.org/10.21468/SciPostPhysCore.6.3.056
33. Dotsenko, V., Maciolek, A., Oshanin, G., Vasilyev, O., Dietrich, S.: Current-mediated synchronization of a pair of beating non-identical flagella. New J. Phys. **21**(3), 033036 (2019). https://doi.org/10.1088/1367-2630/ab0a80
34. Cerasoli, S., Dotsenko, V., Oshanin, G., Rondoni, L.: Asymmetry relations and effective temperatures for biased brownian gyrators. Phys. Rev. E **98**, 042149 (2018). https://doi.org/10.1103/PhysRevE.98.042149
35. Cerasoli, S., Dotsenko, S., Oshanin, G., Rondoni, L.: Time-dependence of the effective temperatures of a two-dimensional brownian gyrator with cold and hot components. J. Phys. Math. Theo. **54**(10), 105002 (2021). https://doi.org/10.1088/1751-8121/abe0d6
36. Tyagi, N., Cherayil, B.J.: Thermodynamic asymmetries in dual-temperature brownian dynamics. J. Stat. Mech. Theo. Exp. **2020**(11), 113204 (2020). https://doi.org/10.1088/1742-5468/abc4e4
37. Viot, P., Argun, A., Volpe, G., Imparato, A., Rondoni, L., Oshanin, G.: Destructive effect of fluctuations on the performance of a Brownian gyrator (2023). https://doi.org/10.48550/arXiv.2307.05248
38. du Buisson, J.: Dynamical large deviations of diffusions, Ph.D. thesis, (Stellenbosch, South Africa, 2022). (2022). arxiv:2210.09040
39. Buisson, J., Touchette, H.: Dynamical large deviations of linear diffusions. Phys. Rev. E **107**, 054111 (2023). https://doi.org/10.1103/PhysRevE.107.054111
40. Argun, A., Soni, J., Dabelow, L., Bo, S., Pesce, G., Eichhorn, R., Volpe, G.: Experimental realization of a minimal microscopic heat engine. Phys. Rev. E **96**, 052106 (2017). https://doi.org/10.1103/PhysRevE.96.052106
41. Li, J., Horowitz, J.M., Gingrich, T.R., Fakhri, N.: Quantifying dissipation using fluctuating currents. Nat. Commun. **10**(1), 1666 (2019). https://doi.org/10.1038/s41467-019-09631-x
42. Sou, I., Hosaka, Y., Yasuda, K., Komura, S.: Nonequilibrium probability flux of a thermally driven micromachine. Phys. Rev. E **100**, 022607 (2019). https://doi.org/10.1103/PhysRevE.100.022607
43. Masoliver, J., Porrà, J.M.: Exact solution to the mean exit time problem for free inertial processes driven by gaussian white noise. Phys. Rev. Lett. **75**, 189–192 (1995). https://doi.org/10.1103/PhysRevLett.75.189
44. Masoliver, J., Porrà, J.M.: Exact solution to the exit-time problem for an undamped free particle driven by gaussian white noise. Phys. Rev. E **53**, 2243–2256 (1996). https://doi.org/10.1103/PhysRevE.53.2243
45. Bray, A.J., Majumdar, S.N., Schehr, G.: Persistence and first-passage properties in nonequilibrium systems. Adv. Phys. **62**(3), 225–361 (2013). https://doi.org/10.1080/00018732.2013.803819
46. Burkhardt, T.W.: First passage of a randomly accelerated particle. In: Metzler, R., Oshanin, G., Redner, S. (eds.) First-Passage Phenomena and Their Applications, pp. 21–44. World Scientific, Singapore (2014). https://doi.org/10.1142/9104 . (**Chap. 2**)
47. Bicout, D.J., Burkhardt, T.W.: Absorption of a randomly accelerated particle: gambler's ruin in a different game. J. Phys. A: Math. General **33**(39), 6835 (2000). https://doi.org/10.1088/0305-4470/33/39/301
48. Levernier, N., Bénichou, O., Guérin, T., Voituriez, R.: Universal first-passage statistics in aging media. Phys. Rev. E **98**, 022125 (2018). https://doi.org/10.1103/PhysRevE.98.022125
49. Capała, K., Dybiec, B.: Random acceleration process on finite intervals under stochastic restarting. J. Stat. Mech. Theo. Exp. **2021**(8), 083216 (2021). https://doi.org/10.1088/1742-5468/ac1664
50. Santra, I., Ajgaonkar, D., Basu, U.: The dichotomous acceleration process in one dimension: position fluctuations. J. Stat. Mech. Theo. Exp. **8**, 083201 (2023). https://doi.org/10.1088/1742-5468/ace3b5
51. Cornell, S.J., Swift, M.R., Bray, A.J.: Inelastic collapse of a randomly forced particle. Phys. Rev. Lett. **81**, 1142–1145 (1998). https://doi.org/10.1103/PhysRevLett.81.1142

52. Swift, M.R., Bray, A.J.: Survival-time distribution for inelastic collapse. Phys. Rev. E **59**, 4721–4724 (1999). https://doi.org/10.1103/PhysRevE.59.R4721
53. Burkhardt, T.W.: The random acceleration process in bounded geometries. J. Stat. Mech. Theo. Exp. **2007**(07), 07004 (2007). https://doi.org/10.1088/1742-5468/2007/07/P07004
54. Burkhardt, T.W.: Chapter. First Passage of a Randomly Accelerated Particle, pp. 21–44. https://doi.org/10.1142/9789814590297_0002. https://www.worldscientific.com/doi/abs/10.1142/9789814590297_0002
55. Basu, U., Majumdar, S.N., Rosso, A., Schehr, G.: Active brownian motion in two dimensions. Phys. Rev. E **98**, 062121 (2018). https://doi.org/10.1103/PhysRevE.98.062121
56. Santra, I., Basu, U., Sabhapandit, S.: Active brownian motion with directional reversals. Phys. Rev. E **104**, 012601 (2021). https://doi.org/10.1103/PhysRevE.104.L012601
57. Woillez, E., Kafri, Y., Gov, N.S.: The active trap model. Phys. Rev. Lett. **124**, 118002 (2020). https://doi.org/10.1103/PhysRevLett.124.118002
58. Wexler, D., Gov, N., Rasmussen, K., Bel, G.: Dynamics and escape of active particles in a harmonic trap. Phys. Rev. Res. **2**, 013003 (2020). https://doi.org/10.1103/PhysRevResearch.2.013003
59. Valageas, P.: Statistical properties of the Burgers equation with brownian initial velocity. J. Stat. Phys. **134**(3), 589–640 (2009). https://doi.org/10.1007/s10955-009-9685-5
60. Dean, D.S., Majumdar, S.N., Schawe, H.: Position distribution in a generalized run-and-tumble process. Phys. Rev. E **103**, 012130 (2021). https://doi.org/10.1103/PhysRevE.103.012130
61. Burkhardt, T.W.: Semiflexible polymer in the half plane and statistics of the integral of a brownian curve. J. Phys. A: Math. General **26**(22), 1157 (1993). https://doi.org/10.1088/0305-4470/26/22/005
62. Bicout, D.J., Burkhardt, T.W.: Simulation of a semiflexible polymer in a narrow cylindrical pore. J. Phys. A: Math. General **34**(29), 5745 (2001). https://doi.org/10.1088/0305-4470/34/29/301
63. Lifshits, I.M., Gredeskul, S.A., Pastur, L.A.: Introduction to the Theory of Disordered Systems. Wiley-VCH, New York (1988). https://doi.org/10.1007/BF02450553
64. Mejía-Monasterio, C., Oshanin, G., Schehr, G.: First passages for a search by a swarm of independent random searchers. J. Stat. Mech. Theo. Exp. **6**, 06022 (2011). https://doi.org/10.1088/1742-5468/2011/06/P06022